The mechanisms that determine the response of the Northern Hemisphere's stationary waves to North American Ice Sheets.

William H.G. Roberts, *

Geography and Environmental Sciences, Northumbria University, Newcastle, UK

BRIDGE, School of Geographical Sciences, University of Bristol, Bristol, UK

Camille Li,

Geophysical Institute, University of Bergen, Bergen, Norway

Bjerknes Centre for Climate Research, University of Bergen, Bergen, Norway

Paul J. Valdes

BRIDGE, School of Geographical Sciences, University of Bristol, Bristol, UK

* *Corresponding author address:*

E-mail: william.roberts@northumbria.ac.uk

ABSTRACT

Stationary waves describe the persistent meanders in the west-east flow of the extratropical atmosphere. Here, changes in stationary waves caused by ice sheets over North America are examined and underlying mechanisms discussed.

Three experiment sets are presented showing the stationary wave response to the albedo or topography of ice sheets, as well as the albedo and topography in combination, as the forcings evolve from 21ka to 10ka.

It is found that although the wintertime stationary waves have the largest amplitude, changes due to an ice sheet are equally large in summer and winter.

In summer, ice sheet albedo is the dominant cause of changes: topography alone gives an opposite response to realistic ice sheets including albedo and topography.

In winter, over the Atlantic, stationary wave changes are due to the ice sheet topography; over the Pacific, they are due to the persistence of summertime changes, mediated by changes in the ocean circulation.

It is found that the response of stationary waves over the last deglaciation echoes the above conclusions, with no evidence of abrupt shifts in atmospheric circulation. The response linearly weakens as the albedo and height decrease from 21ka to 10ka.

As potential applications, the seasonal cycle over Greenland is shown to be sensitive primarily to changes in summer climate caused by the stationary waves; the annual mean circulation over the North Pacific is found to result from summertime, albedo-forced, stationary wave effects persisting throughout the year because of ocean dynamics.

1. Introduction

The seasonally averaged circulation of the Earth's atmosphere at middle latitudes is characterised by a meandering west to east flow. The meanders or "stationary waves" have been a subject of research for the many decades since they were first described and their underlying physics explored (Charney and Eliassen 1949; Bolin 1950; Smagorinsky 1953). By separating the full complexity flow into a uniform west to east component with a wavy component superposed on top, it is possible to reduce the system into more understandable elements. This philosophy for reducing the complexity of a system into tractable elements has been further applied to understanding the wavy part of the flow, isolating the role that heating or topography may play in exciting the stationary waves (see for example the review of Held et al. 2002). Decomposing the flow into simple elements not only leads to a mathematically simpler analysis, but also allows one to build up an intuition for how to conceptually describe the flow. In this paper we shall use a similar philosophy to describe how the stationary waves evolve in response to ice sheet forcing, focusing on the role that ice sheet albedo and topography play. Although we shall spend much of the paper describing one state of the ice sheet, by understanding how these elements interplay we shall be able to gain an intuition for describing how the stationary waves will differ for any state of the ice sheet. Such an intuition is extremely powerful for understanding paleoclimate proxy data which vary in time.

Attempting to understand the role that different glacial boundary conditions, and particularly those of the Laurentide and Cordilleran Ice Sheets (LCIS), play in altering the atmospheric circulation is not a new idea (e.g. Cook and Held 1988). Many studies have focused upon the wintertime stationary waves. These studies have generally shown that the response to the topography of the ice sheet is the most important (e.g. Broccoli and Manabe 1987; Cook and Held 1988; Kageyama and Valdes 2000; Pausata et al. 2011; Hofer et al. 2012; Löfverström et al. 2014). However, although the amplitude of the stationary waves is largest in winter (e.g. Peixoto et al. 1992; Hartmann 1994), it is not obvious that

changes to the stationary waves will also be largest in this season. Furthermore, if we wish to understand the signals captured by proxies that recorded the climate of the past, it is important to understand what causes changes to the climate in seasons other than winter, since these proxies often reflect these different seasons. In this paper we therefore consider in detail the extreme seasons of both summer and winter. As we shall show, the responses to ice sheet forcing are quite different in these two seasons.

A dynamic ocean can also play an important role in the response of the stationary waves. Many previous studies have used atmosphere-only simulations with fixed SST (e.g. Hofer et al. 2012; Merz et al. 2015; Löfverström and Liakka 2016) or slab oceans (e.g. Cook and Held 1988, 1992; Löfverström et al. 2014). While a specified SST allows one to isolate a single forcing, it neglects a crucial feedback. Slab oceans go part of the way to capturing the role of the ocean, but it is only with all of the relevant dynamics that the role of the ocean can really be captured. Yanase and Abe-Ouchi (2010) showed that in response to ice sheet forcing, the response over the Pacific was highly variable when models without a dynamic ocean were used; models with a dynamic ocean were quite consistent in their response. Exactly how the dynamic ocean might cause this is most easily demonstrated by using identical atmosphere models coupled to either fixed SST or to a dynamic ocean. This is the approach that we take.

While understanding how the stationary waves respond to the largest, Last Glacial Maximum (LGM), ice sheets is important, understanding how smaller ice sheets influence the climate is just as important: during the majority of the last glacial period the ice sheets were much less extensive than at the LGM, 21kyr ago. A number of studies have looked at specific cases of different ice sheets (Ullman et al. 2014; Löfverström et al. 2014; Merz et al. 2015), and have shown that the stationary waves do differ with these different ice sheets. To understand these differences the focus has generally been on the different topography of the ice sheets and its mechanical forcing, not on the area of the ice sheet and its diabatic forcing. Since in summer this diabatic forcing is especially important (Ting 1994), if we are to

correctly understand how the stationary waves evolve, understanding the role of albedo can not be omitted. Indeed the relative role of albedo and topography needs to be understood to fully appreciate how the stationary waves might have evolved in the past. In this way we can understand periods when ice sheet area and topography might have been different, yet total ice volume the same. In addition, while it is helpful to understand the details of the response to specific ice sheets, it is also helpful to understand in more general terms how the climate may respond to ice sheets of any size. Many climate proxy records are continuous and therefore reflect a continuum of ice sheet configurations. Since it is still rare to be able to simulate the response of the climate to such continuously evolving boundary conditions, having a general understanding of how the stationary waves evolve in response to a range of ice sheet configurations allows one to place proxy records in the context of a response to an evolving ice sheet, without explicit simulation. In this study we shall use a number of different simulations to understand when ice sheet albedo is the most important forcing, when topography is the most important, and how the response varies with incrementally different ice sheet size. In this way we can more generally understand the role that ice sheets play in the climate system and place continuous proxy records into this context.

This paper proceeds as follows. In Section 2 we describe the model configurations that we use. In Sections 3 and 4 we describe in detail how the stationary wave patterns change in response to the largest, 21ka, ice sheet configurations. In these sections we open the discussion by describing these responses and comparing them to previous studies before analysing the response in the context of known dynamical processes. In Section 5 we describe how the stationary waves evolve with a set of ice sheet reconstructions of the Last Deglaciation, from 21ka to 6ka. In Section 6 we place our results in the context of other studies of stationary waves of the ice age climate, in Section 7 we describe how our results may be used to place palaeoclimate records into a wider context. Finally we conclude in Section 8.

2. Simulations

We analyse simulations using both coupled and atmosphere-only models. With these two set ups we can isolate where significant feedbacks arise from changes in the ocean circulation. Since many of the early studies examining the impact of ice sheets on the atmosphere's stationary waves lacked a dynamic ocean, understanding the role that the ocean may play is important for extending the findings of these studies.

We use the atmosphere-only general circulation model HadAM3 (Pope et al. 2000; Valdes et al. 2017) and its coupled atmosphere and ocean counterpart HadCM3 (Gordon et al. 2000; Valdes et al. 2017). Specifically we use the HadAM3B-M1 and HadCM3B-M1 versions reported by Valdes et al. (2017). These model configurations are similar to those in the original references but contain a number of bug fixes and, most importantly for this study, the atmosphere component in HadCM3B-M1 is identical to that in HadAM3B-M1. Changes in the stationary wave behaviour between the coupled and atmosphere-only simulations can, therefore, only arise from the presence or absence of a dynamic ocean. The coupled simulations of HadCM3 that we use were previously reported by Roberts and Valdes (2017).

At the LGM the greenhouse gas concentrations were different, with the carbon dioxide concentration notably lower; ice sheets present over North America and Eurasia; the orbital configuration different, though very similar to today. A full LGM simulation therefore requires changes to all of these parameters (Kageyama et al. 2017). Such a simulation is needed to compare with proxy data, however for a mechanistic understanding of the climate it is far from ideal. Changing many boundary conditions at once means that it is very difficult to know which of the boundary conditions causes any change. Changing one forcing at a time allows one to diagnose the exact role of that forcing. Many previous studies have shown that it is the topography of the ice sheets that has a dominant influence on the North Atlantic mid-latitude circulation (e.g. Broccoli and Manabe 1987; Cook and Held 1988; Kageyama and Valdes 2000; Pausata et al. 2011; Hofer et al. 2012; Löfverström et al. 2014). Greenhouse gas concentrations can have an impact at mid-latitudes though the changed meridional tem-

perature gradient that they imply, this effect is however secondary (Broccoli and Manabe 1987).

To describe the boundary conditions that we use, we quote from Roberts and Valdes (2017): *We derive our boundary conditions from the ICE-5G (VM2) reconstruction of the ice sheets (Peltier 2004). Unless otherwise indicated, boundary conditions are for the pre-industrial. This includes the greenhouse gases and orbital forcing and the land sea mask. Of course, over the Last Deglaciation all of these forcings changed, but it is not our intention to make the best simulation of the Last Deglaciation rather to understand how an ice sheet impacts the climate. We simulate timeslices every 1ka from 21ka until 6ka.*

To investigate the effect of albedo (experiment ALB), land areas that are ice covered at each timeslice have all of their surface properties set to those of land ice. These include surface albedo and roughness, and all of the model's other vegetation and soil parameters. We impose this land surface change to all ice covered areas in the Northern Hemisphere, so include changes in the albedo over both North America, where the LCIS lay, and over Northern Europe, where the Eurasian Ice Sheet lay. In this way we create a time varying "White Plain" in the NH.

To investigate the role of topography (experiment TOP), land areas in which the LIS existed have their surface topography raised to be that of the ICE-5G reconstruction. We add this surface elevation change as an anomaly to the pre-industrial topography that is used in control runs of HadCM3. We only change the surface topography over North America, everywhere else remains as in the pre-industrial. We therefore ignore the effect of the Eurasian Ice Sheet's topography. Due to its larger size the LIS has a much larger impact on the climate than the Eurasian Ice Sheet. All other surface properties remain the same as for the pre-industrial. It should be noted that over time, due to the increased elevation of the surface, snow does accumulate on top of the topography anomaly causing a small albedo anomaly. It can be seen [Figs. 9b and 9d of Roberts and Valdes (2017)] *that there is a small change in the ice sheet area in experiment TOP; the figures also show that this change is a tiny*

fraction of the change in the albedo that arises from the imposition of an ice sheet. With these changes in the surface properties we create a "Green Mountain".

Finally to investigate the role of topography and albedo (experiment ALB/TOP) we combine the boundary condition changes of experiments ALB and TOP. We therefore have a land surface that simulates land ice, and its associated change in albedo, everywhere that was ice covered in the NH at each time slice (including over Eurasia), and a topography that is raised over North America (but not over Eurasia). In this way we create a "White Mountain".

The SST boundary condition used in the atmosphere-only simulations are taken from a pre-industrial control simulation of the coupled model. For the detailed analysis of the 21ka stationary waves shown in Sections 3 and 4 we use the long simulations (700 years: ALB, TOP; 900 years: ALB/TOP) and for the analysis of the evolution of the patterns in Section 5 we use the shorter simulations (200 years: ALB; 500 years TOP, ALB/TOP). At the end of the longer runs the net TOA energy imbalance is approximately 0.3 Wm^{-2} in all simulations. This indicates that the runs are well spun up: for comparison the PMIP2 simulations used in many studies of the past climate have TOA energy imbalances of between 0.2 and 1.6 Wm^{-2} (Donohoe et al. 2013). Analysis is undertaken on means from the final 100 years of the simulations. For a fuller discussion of how close to equilibrium our simulations are we refer the reader to Roberts and Valdes (2017).

Figure 1 compares the stationary waves simulated by HadCM3 and HadAM3 with those derived from the ERA interim reanalysis data (European Centre for Medium-Range Weather Forecasts 2012). We plot the eddy geopotential height at two pressure levels: 850hPa and 200hPa. With these 2 levels we can assess the vertical structure of the patterns, and through this understand the forcing mechanism of the waves. Comparing the winter, DJF, patterns we see that the simulated patterns are very similar to those seen in the reanalysis data in terms of both the spatial patterns and their amplitudes. There are a set of ridges and troughs with an equivalent barotropic structure over North America extending far over the

North Atlantic and into Asia. Over the Pacific there is a deep equivalent barotropic trough. In summer, JJA, the patterns are again very similar in the models and reanalysis data, although the model simulated stationary waves are rather stronger in amplitude than those seen in the reanalysis data. Spatially, the models and reanalysis show a series of baroclinic structures with surface ridges and upper level troughs over the Pacific and Atlantic oceans. Since the models replicate the vertical and horizontal structure of the stationary waves seen in the reanalysis data, we suggest that the models are not only capable of simulating the stationary waves themselves, but are also capable of simulating the mechanisms that cause them. For example, the baroclinic structures seen in JJA suggest that the models are correctly simulating the stationary waves as a response to heating rather than mechanical forcing. We feel confident, therefore, that the models can correctly simulate the processes that shall be crucial for understanding how the stationary waves evolve in response to the presence of ice sheets. It is to this that we now turn our attention.

3. Wintertime stationary waves

In the modern climate, the wintertime stationary waves are a response to the mechanical forcing from topography as well as the dynamical forcing form diabatic heating due to transients and the flow over the topography (Valdes and Hoskins 1989; Nigam et al. 1986, 1988; Held et al. 2002). Simple linear models have shown that during glacial times the response of the stationary waves to an ice sheet is rather less complicated and can be considered as simply the mechanical response to the topography of the ice sheet (Cook and Held 1988).

In Fig. 2(a,d), which shows the difference between experiment ALB and the control in winter, we see that the impact of ice sheet albedo on the stationary waves is small. Considering the atmosphere-only response (a), we see small changes in the 200 hPa height field but no noticeable change at 850 hPa. The coupled response (d) is larger both aloft and near the surface. The most notable feature is a small surface and upper level trough over

the Bering Sea. The overall small response is unsurprising, since there is little to force a change. The wintertime stationary waves have been shown to be a response to topographic forcing (e.g. Valdes and Hoskins 1989; Nigam et al. 1986, 1988; Held et al. 2002) and in ALB the topography is no different to the control simulation. The stationary waves are also a response to diabatic heating, but this also does not change: in NH winter much of the area that is ice covered in ALB is snow covered in the control simulation, resulting in a negligible change in the surface albedo. The response in the Bering Sea in the coupled simulation is the result of a cold surface temperature anomaly in this region. This arises from the change in the summer time circulation that shall be detailed in the following section.

The response of the wintertime stationary waves to the Green Mountain's topography, shown by experiment TOP, is large both upstream and downstream of the ice sheet (Fig. 2(b,e)). Looking first at the atmosphere-only response we see an upper level trough over the ice sheet. This trough is centred to the east of the highest heights of the ice sheet. Farther downstream of the ice sheet we see ridges both equatorward and poleward of this trough. This response is consistent with the linear response to ice sheet topography described at length by Cook and Held (1988). Indeed, as suggested by linear models, in TOP the equatorward ridge is more prominent than the poleward ridges and troughs. In the coupled simulation (Fig. 2(e)) we see a generally larger response than in the atmosphere-only simulation. The trough over the ice sheet in the coupled simulation is deeper and extends farther east over the North Atlantic; the 850 hPa response in the North East Atlantic is also far larger. Interestingly, however, the ridge that is equatorward and downstream of the ice sheet is weaker throughout the atmosphere in the coupled simulation. This weakening of the response is consistent with a more non-linear response of the atmospheric flow, unsurprising since the coupling of the atmosphere to the ocean introduces significant non-linearities to the climate system.

Upstream of the ice sheet in the atmosphere-only simulations there is an upper and lower level ridge to the the west of the ice sheet, centred over the Bering Strait. To the west and

south of the ice sheet there is an upper level trough, centred near 35°N, 190°E. The ridge feature is very similar to the linear response shown by Cook and Held (1992). When the coupled model is used the upper level ridge due west of the ice sheet remains, with the near surface expression much enhanced in the sea of Okhotsk. The upper level trough centred at 35°N, 190°E is somewhat deepened by the inclusion of a dynamic ocean.

The response to the combined albedo and topography of the White Mountain in experiment ALB/TOP is shown in Fig. 2(c,f). Looking first at the atmosphere-only response we see striking similarities between ALB/TOP and TOP (Fig. 2(e)), but with a generally larger response in ALB/TOP. This difference in the response, both up and downstream of the ice sheet, is because of a diabatic cooling over the ice sheet in ALB/TOP compared to TOP.

In the coupled simulation the response during winter downstream of the ice sheet in ALB/TOP is very similar to that in TOP. The most notable differences are upstream, where in ALB/TOP there is a large upper and lower level trough centred near 35°N, 190°E and an upper level ridge centred over 20°N, 220°E. These features are only apparent in the coupled simulation, therefore are a direct response to ocean feedbacks. Comparing ALB and ALB/TOP (Figs. 2(d) and (f)), these same features are apparent in both simulations indicating that they are a response to the surface albedo. These features are associated with colder surface temperatures in the mid North Pacific that are established during the summer months. In ALB/TOP, because of the topographically forced ridge over Beringia, this North Pacific feature is located somewhat to the south of that in the ALB simulation.

The response shown in these model simulations is very similar to the response to the ice sheet forcing shown by Manabe and Broccoli (1985) and analysed by Cook and Held (1988). The trough over the ice sheet shown by Manabe and Broccoli (1985) is displaced to the east of that shown in Fig. 2(c,f). This is consistent with the different ice sheet topography used in their study which has its highest heights farther to the east of those in ICE-5G. The ridges downstream of the ice sheet are similarly located farther east in their simulations. The importance of topography was highlighted by Ullman et al. (2014). Using the same model

but 2 different ice sheet topographies, they showed that the ice sheet with higher elevations in the east has its stationary wave response shifted to the east.

The role that the ocean plays in setting the change in the stationary waves can be seen by comparing the top and bottom rows of Fig. 2. Including a dynamic ocean enhances the stationary wave response especially near the surface. It also changes slightly the response in the TOP and ALB/TOP experiments, especially upstream and far downstream of the ice sheet. In these regions the different SST patterns that result from the different ice sheets can alter the stationary waves. In particular the wintertime stationary wave over the North East Atlantic is significantly enhanced with a dynamic ocean and, in turn, the atmospheric response downstream of this region, over Asia, is enhanced.

4. Summertime stationary waves

In the modern climate, the Northern Hemisphere summertime stationary waves have been shown to be a response to diabatic heating (Ting 1994). This diabatic heating can be a direct result of surface heating (Rodwell and Hoskins 2001) or an indirect result of a flow that is ascending or descending some topography (Ting 1994). How the summer stationary waves differ in a glacial climate has received little attention, however. Ringler and Cook (1999) showed that in an idealised model set up to mimic an ice sheet, the interaction between topography and diabatic heating is complex and does not fit well within a simple linear framework.

The summertime stationary wave response to a White Plain in experiment ALB is large both up and downstream of the ice sheet (Fig. 3(a,d)). The pattern of the response is similar in both the atmosphere-only and coupled simulations, although the response is slightly reduced in the coupled simulation, especially far downstream over Siberia. The large response in this season can be understood in terms of the change in the diabatic heating that arises from the white surface (Fig. 4). In summer the prescribed ice cover over North America

in experiment ALB dramatically increases the surface albedo. This causes a large cooling anomaly over North America. In contrast during winter, when much of North America is snow covered in the control simulation, prescribing ice cover has a limited impact. Furthermore, during summer when the mean zonal wind speed is weaker, the stationary waves are more influenced by heating (Ting 1994).

Downstream of the ice sheet the atmospheric response is broadly similar to the deep heat source at mid-latitudes case of Hoskins and Karoly (1981). Figure 5 shows that immediately downstream of the heating there is a strong baroclinic response with a surface ridge and upper level trough (the reverse of Hoskins and Karoly (1981) since the White Plain gives a cooling rather than heating). Farther downstream there are ridges that extend throughout the atmosphere with minimal tilt (Hoskins and Karoly 1981; Held 1983).

Upstream of the ice sheet the summertime response can again be interpreted as the response to the implied heating anomaly. Rodwell and Hoskins (2001) showed that the intensity of the subtropical high in the Pacific during summer is strongly influenced by the heating that occurs over North America during that season. With the reduced heating from the White Plain, there is a reduction in the strength of the low level subtropical high and a concomitant decrease in the strength of the upper level trough. The change in the surface pressure resulting from the ice sheet albedo was also shown by Yanase and Abe-Ouchi (2010). In the control simulation, the largest heating is seen around 40°N, and the summertime surface subtropical high is located near this latitude; the anomalous diabatic cooling introduced by the White Plain is to the north of this, near 50-60°N, and the anomalous surface trough is also located near 50-60°N, to the north of the control simulation's subtropical high. There is a remarkably small difference between the coupled and uncoupled atmospheric response to the White Plain indicating that ocean dynamics are minimally important in causing this feature. By contrast in winter it is only in the coupled simulation that the changes in the North Pacific manifest themselves. We therefore propose that in experiment ALB the summer time heating anomaly causes a change in the surface ocean that, while minimally important in

changing the flow in the summer season, is crucially important in changing the wintertime circulation.

The response of the stationary waves to a Green Mountain in experiment TOP during summer is also large (Fig. 3(b,e)). There is a large upper level ridge that sits atop the highest topography, with a series of troughs and ridges downstream of the ice sheet. The first comparison to make is between the summer and winter time responses. Broadly, the JJA response to the Green Mountain is opposite to that in DJF. This implies that the mechanisms by which the topography forces the stationary waves in TOP during JJA are not the same as those in DJF: in experiment TOP during JJA the stationary waves are not merely responding to the mechanical forcing of the topography. Downstream of the ice sheet there is an upper level trough that has its maximum just to the south of Greenland. There is a similar feature in ALB, however the trough in TOP is to the east of that in ALB. This reflects the rather different cause of this feature in TOP. In ALB the upper level trough is a direct response to the diabatic heating and sits closer to the ice sheet itself; in TOP the trough is a downstream response to the topography and sits downstream of the ice sheet. This can most easily be seen in vertical sections of eddy geopotential height. In ALB (Fig. 5(a)) the upper level trough is over the eastern edge of the ice sheets: in TOP (Fig. 5(b)) it is centred 20° east of the eastern edge. These differences shall be important when we consider the response to a White Mountain.

Upstream of the ice sheet the response in TOP displays a distinctive baroclinic structure, suggesting that it is a local response to diabatic heating (Ting 1994). The anomalous ridge/trough features are located to the north of the control simulation's which is consistent with the more northward position of the diabatic heating anomalies (Fig. 4). This response is similar to that seen in ALB but with a reversed sign: in TOP the topography introduces a positive heating anomaly in contrast to the negative heating anomaly in ALB.

Comparing the coupled and atmosphere-only simulations, we see that the climate's response downstream is somewhat weakened, as was the case in the White Plain experiment.

Upstream of the ice sheet the response is significantly enhanced by the interactive ocean. In all experiments the presence of the interactive ocean tends to increase the heating over the continent relative to the atmosphere-only experiment. Since the presence of the Green Mountain increases the heating over the continent, including the interactive ocean further increases this heating, with a concomitant increase in the strength of the response upstream and decrease downstream.

The response in experiment ALB/TOP during summertime is most similar to ALB, and in general is opposite to that seen in TOP (Fig. 3(c,f)). Directly over the White Mountain's topography there is a weak ridge at the surface and upper levels (Fig. 5(c)). There is a surface ridge over the ice sheet in ALB (Fig. 5(a)), however this is very much a surface feature. We shall argue later that the upper level ridge is a mechanical response to topography. Finally, the opposite responses in experiments TOP and ALB/TOP suggest that understanding the processes by which a Green Mountain influences stationary waves is not relevant to understanding the last ice age, which had White Mountains.

In the atmosphere-only simulation, downstream of the ice sheet there are a series of ridges and troughs. These are located in positions more reminiscent of ALB than TOP, especially in the case of the first downstream trough which peaks over the eastern edge of the ice sheet. Farther downstream, the ridge over the eastern Atlantic is located slightly equatorward of that in either ALB or TOP. Upstream of the ice sheet there is little difference between the response in ALB/TOP and ALB. There is a ridge that forms over Alaska in ALB/TOP which is not present in ALB and also a ridge over Central Russia, however the largest response, over the Pacific ocean, is the same in both simulations. The response in the coupled simulation is very similar to that in the atmosphere-only simulation, with only a slight reduction in the amplitude of the response apparent in the coupled simulation.

The similarities between ALB and ALB/TOP can be best understood in terms of the heating field which is similar in the ALB and ALB/TOP experiments and opposite to that in TOP. Figure 4 shows the implied diabatic heating from the different ice sheets. The

Green Mountain causes a positive diabatic heating anomaly on the downstream side of the ice sheet (Fig. 4(b)). This is associated with the ridge that we showed sits atop the ice sheet. These features are consistent with the response to topographic forcing of a westerly flow in a baroclinic atmosphere described by Hoskins and Karoly (1981) in their Fig. 7(c). This response is not the same as the equivalent barotropic vertical response to topography which describes the winter circulation (see previous section). Nor is it similar to either the White Plain (Fig. 4(a)) or White Mountain (Fig. 4(c)) both of which cause a negative diabatic heating anomaly over the ice sheet in summer. The amplitude of the heating anomaly in both ALB and ALB/TOP is similar in the two cases. It is, therefore, unsurprising that the upstream response of the climate, which is the most directly influenced by the heating, is very similar in these two experiments. These similarities can be emphasised by plotting the difference between ALB and ALB/TOP (Fig. 6). In the atmosphere-only simulation, over the Pacific there is no change in the stationary wave pattern (not shown); in the coupled simulation the changes are small (Fig. 6(a,c)). The region where topography is important is over Alaska. Here a ridge forms when the topography is raised; this ridge also forms in the TOP experiment, indicating that diabatic heating is not important in establishing this feature.

Downstream of the ice sheet similar arguments apply. Hoskins and Rodwell (1995) and Ting (1994) both showed that during summer most of the atmosphere's stationary wave features could be explained using simplified atmospheric models forced only by the diabatic heating pattern. Including the topography had only a small effect. These simulations used the modern topography, rather than the LGM ice sheets used in this study. In our simulations we find a larger role for topography downstream of the ice sheet. Figure 6 shows the additional changes in the stationary waves that arise from elevating a White Plain to a White Moutain. There is a striking similarity between the difference between experiments ALB/TOP and ALB in JJA (Fig. 6 a,c) and TOP and the control in DJF (Fig. 6 b,d). In the preceding section we argued that in DJF the response of the stationary waves to topography

(shown by experiment TOP) could be considered in terms of the response to the mechanical forcing of the ice sheet. We therefore argue that the additional effect of elevating a White Plain in JJA can also be considered as the simple response to the mechanical forcing of the ice sheet. There are differences, however. The response of the raised elevation in JJA is weaker than the mechanically forced response in DJF, and the equatorward upper level ridge downstream of the ice sheet is farther east in the elevated White Plain.

The location of this ridge may be explained by the different mean state conditions in JJA compared to DJF and their impact on the propagation of planetary waves (Hoskins and Ambrizzi 1993). Figure 7 shows maps of the stationary wavenumber in the White Mountain simulation for DJF (a) and JJA (b). We see that during the winter the waveguide has a much larger latitudinal extent than during the summer. This means that during the winter, waves excited by the ice sheet topography can propagate deeper into the tropics. During the summer, by contrast, waves excited by the topography are constrained by the narrower waveguide and propagate more zonally. Figure 6(a) shows this with the upper level ridge in JJA being centred near 40°N, 30°W (panel (a)), and in DJF the same feature being centred near 30°N, 60°W (Fig 6(b)). This same argument can be applied to the other downstream ridges and troughs that are a response to the topography, which all propagate more zonally in summer than in winter. The largest changes in the waveguide are seen between the JJA and DJF seasons (Fig. 7(c,d)), however there are differences in the waveguides within the same season caused by the different ice sheets. In the winter the ice sheet topography lowers the average wavenumber to the south of the ice sheet allowing for the propagation of lower wavenumbers in this region. The ice sheet albedo has a negligible effect. By contrast in summer, the ice sheet albedo causes a similar lowering of the stationary wavenumber to the south of the ice sheet, the topography alone causes, if anything an increase in the average wavenumber.

We conclude that the summertime response to a White Mountain in experiment ALB/TOP can be considered as the combined response to the reduced diabatic heating, caused by the

reduced albedo, and the mechanical forcing of the raised topography. This response can not be considered the linear combination of the ALB and TOP simulations.

5. Stationary wave evolution over the last 21kyr

In the previous sections we described the details of the atmosphere's response to the different elements of an ice sheet, for an ice sheet at the glacial maximum. In this section we shall describe how the atmosphere responds to smaller ice sheets. We shall use the sets of simulations described by Roberts and Valdes (2017). These are simulations that cover the period 21–6ka using the fully coupled HadCM3 model forced by the different elements of the ice sheets. The simulations described in the previous section are the 21ka simulations from this set.

To describe how the stationary waves evolve we shall compute the EOFs of the 200 hPa height field for the 15 simulations in each set. Since in the preceding section we found rather different responses up and downstream of the ice sheet, we compute 2 EOFs for these simulations, one upstream of the ice sheet (120°W-60°E, 10°N-85°N) and one downstream (60°E-240°E, 10°N-85°N). In order to relate these time evolving patterns to the analysis of the previous section we also compute the pattern correlations between the EOFs and the response patterns at 21ka (Table 1). High pattern correlations indicate similar mechanisms are at work. Plotting the EOFs (Figs. 8 and 9) gives spatial information about the atmospheric response to ice sheet evolution; to understand the temporal evolution we project the EOFs onto the underlying 200 hPa height fields to obtain time series of the EOFs principal components. Since we are interested less in how the stationary waves respond in real time than we are interested in how they respond to the size of the ice sheet, we plot these PCs against metrics of the ice sheets area and height (Fig. 10 and 11). Finally, since we wish to understand how the stationary waves from a White Mountain can be related to their constituent albedo and topography responses, we project the EOFs from the ALB and TOP

set of experiments onto the 200 hPa height field from the ALB/TOP set of experiments to understand how well these EOFs explain the combined response. These are plotted as the faint blue circles on the ALB and TOP experiments. We only show the first EOFs since these explain the majority of the variance (Table 1).

Mathematically we can define the principal components (PCs) for each experiment as, for example with ALB,

$$PC[\text{ALB}](t) = Z200[\text{ALB}](x, y, t) \cdot EOF[\text{ALB}](x, y), \tag{1}$$

which means that the projection of the EOFs from ALB onto experiment ALB/TOP is:

$$Projection[\text{ALB}](t) = Z200[\text{ALB/TOP}](x, y, t) \cdot EOF[\text{ALB}](x, y). \tag{2}$$

If the values of $Projection[\text{ALB}](t)$ are similar to those of $PC[\text{ALB}](t)$, then $EOF[\text{ALB}]$ is a good description of the evolution of $Z200[\text{ALB/TOP}]$; if they are not then the EOFs do not capture the evolution.

a. Winter

In ALB we saw little change in the wintertime stationary waves at 21ka and this is consistent through time. In TOP the spatial pattern of the evolving response is very similar to that of the 21ka simulation (Table 1). This is true both upstream (Fig. 8(c)) and downstream of the ice sheet (Fig. 8(d)). Furthermore, we find that the amplitude of the response varies linearly with the increasing height of the ice sheet (Fig 10(e,f)). The pattern of the response to the evolving ice sheet in the ALB/TOP experiments is also much like the response to the 21ka simulation both up and downstream (Fig. 8(e,f)). Again this pattern evolves linearly with the ice sheet height (Fig 10(e,f)). Comparing the influence of albedo and topography in ALB/TOP, we find that in winter there is little influence from albedo at any state of the ice sheet; furthermore, it is remarkable how much of the pattern from the TOP set of experiments can explain the evolution in the ALB/TOP set (Fig 10 e,f light blue dots). This

is true, both up and downstream of the ice sheet. There are small differences in the spatial patterns for the White and Green Mountains: the response in ALB/TOP tends to be larger than in TOP. However, in the hemispheric average these differences are small.

b. Summer

The summer patterns are rather more complex. In the ALB set of simulations the upstream and downstream patterns of evolution are both very similar to the 21ka patterns (Table 1). The upstream and downstream patterns both evolve linearly with increasing ice sheet area (Fig. 11 a,b), although there is some suggestion that the upstream response peaks when the ice sheet area is near 3×10^{13} km^2 (which occurs at 16ka) and does not increase despite the ice sheet being nearly 10% larger than this at 21ka. In TOP the patterns of evolution are also similar to the pattern shown at 21ka. The time evolution of the pattern is not linear: both up and downstream of the ice sheet the response of the atmosphere is weaker for small ice sheets. Indeed, it is only when the mean height of the ice sheet is greater than 0.2 km that there is much of change in the stationary waves upstream of the ice sheet. Maps of the stationary waves for these smaller ice sheets (not shown) show that although there is a response in the atmosphere it is not well matched by the 21ka response.

The response during summer in the ALB/TOP set of experiments is very similar to the 21ka response (Table 1). We first consider the response upstream of the ice sheet. The amplitude of the pattern increases with the increasing size of the ice sheet. However, both the area and height of the ice sheet are important: it can be seen that the increase in amplitude of the principal component (Fig. 11c) with increasing ice sheet area is not linear, indicating that other processes must also be important, furthermore, from 18ka until 21ka when the ice sheet area changes little but the height of the ice sheet continues to increase, the amplitude of the response also continues to increase. This fits with our discussion in the previous section which showed that topography is a contributor to the summer time response in ALB/TOP. Of all of the summertime EOFs, the EOF of the ALB/TOP suite

explains the smallest fraction of the total variance over the period 21-6ka (Table 1). This indicates that the simple framework of one pattern describing the stationary wave's evolution is far less applicable in this experiment, as compared to experiments ALB and TOP. There is little similarity between the response to a Green and White Mountain responses at any state of the ice sheet(Fig. 11(e), green dots and light blue dots respectively); the White Plain pattern, although better, still fails to capture some details of the response, as was highlighted earlier(Fig. 11(a), red dots and light blue dots respectively).

Looking at the response downstream of the ice sheet, a similar picture emerges: ice sheet topography can not explain the evolution of the stationary waves, however the area of the ice sheet, is not the sole determining factor. The pattern of the evolution of the stationary wave is very similar to the pattern of the 21ka stationary wave change.

6. Discussion

In this section we shall place the results that we have presented into the context of previous studies. As we shall discuss, many previous studies have used linear models of the atmosphere in order to understand which are the most important forcing mechanisms. Although we have not used explicitly linear models in our analysis, much of our interpretation uses implicitly linear thinking: we have attempted to explain the response in the ALB/TOP experiments as the superposition of the response in the ALB and TOP experiments. In this way we consider the linearity with respect to the boundary conditions rather than the linearity with respect to the forcing to the climate that these boundary conditions imply. As we have discussed there are occasions when such an interpretation fails. However, we feel that it is a useful way to gain an intuition for how the climate responds to the ice sheets, and so understand how the stationary waves may behave in situations that we have not explicitly simulated.

a. Winter

Cook and Held (1988) and Cook and Held (1992) both investigated how far a linear framework could be taken to explain changes in the ice age stationary waves. They showed that it was capable of explaining a considerable amount of the response. Downstream of the ice sheet our results echo this. Comparing the TOP and ALB/TOP simulations we show that mechanical forcing can explain much of the stationary wave response; examining the evolution of the stationary waves we find that the patterns remain much the same with increasing topographic height and their amplitude increases linearly. Furthermore, the key non linearity introduced by ocean dynamics has only a small effect. Considering the non-linearity introduced by diabatic heating, as suggested by Ringler and Cook (1999), the additional cooling that the white ice sheet surface causes can enhance the mechanical response to topography, while not necessarily changing the pattern. Upstream of the ice sheet, however, non-linearity is far more important.

Yanase and Abe-Ouchi (2010) demonstrated that over the North Pacific the presence of the ice sheet forced trough is the result of ocean dynamics, a result that we also show. This trough is also evident in the annual mean in the simulations of Pausata et al. (2011). It is remarkable how robust this feature is if a dynamic ocean is present. As was highlighted by Yanase and Abe-Ouchi (2010), in atmosphere-only and slab ocean model simulations the response over the North Pacific is highly variable from model to model. By contrast, when a dynamic ocean is used the response is quite consistent. The ridging over the Bering Sea is less sensitive to ocean dynamics, and this feature is also strongly influenced by the height of the ice sheet, a result similar to that shown by Otto-Bliesner et al. (2006) over the annual mean.

Löfverström et al. (2016) have proposed that the strong stationary feature in the North East Atlantic can be considered as a result of the reflection of Rossby Waves into this region caused by the topography of the ice sheet. Although we find a similar feature in our simulations it is much stronger in the coupled model than it is in the atmosphere-only model.

This suggests that this feature is not the result of a change to the waveguide caused by the topography alone, but that other non-linearities, such as changes in the ocean circulation and possible changes in the locally forced Rossby Waves, are also important.

We also considered how the evolving shape of the ice sheets can influence the stationary waves. Ullman et al. (2014) stated that as the shape of the ice sheet changes, so too can the stationary waves. It is not possible to ascertain how much of the change they showed is a change in amplitude and how much a movement in the pattern, so it is not possible to say how much of the change might be understood as a change in the amplitude of a fixed pattern, caused by reduced ice sheet height, and how much is a movement in the pattern itself (as shown for example by Roe and Lindzen 2001). Relatively small changes in the ice sheet topography have been shown to impact the global amplitude of the wintertime stationary waves if these changes are in specific locations (Jackson 2000; Löfverström et al. 2014). We find no evidence for this in our many simulations. In winter time it is only when the height of the ice sheet becomes comparable to the Rocky Mountains that we find a marked change in the stationary wave pattern. The major difference between our study and these previous studies is that we use a fully coupled model. We have shown that changes in the ocean circulation are an important component of the stationary wave response to ice sheet topography, so we suggest that an extreme sensitivity to ice sheet topography may arise from the lack of a dynamic ocean. We therefore propose that in agreement with the earliest studies of ice age stationary waves, the patterns scale linearly with the height of the ice sheet.

b. Summer

The summer time stationary waves have attracted far less attention than those in the winter. Ringler and Cook (1999) examined the interactions between heating and mechanical forcing in a simplified context. They concluded that the interaction of these effects was highly non-linear. Our results agree with this, although we do show that it is to a certain extent

possible to explain the downstream impact of a White Mountain in terms of the heating response to a White Plain and the mechanical impact of the topography. Understanding the amplitude of this latter part is difficult, however.

Upstream of the ice sheet Yanase and Abe-Ouchi (2010) proposed that the response over the North Pacific is the result of heating anomalies over North America, a response that we too find. The ridging to the north of this, over Alaska has been suggested to be associated with the observed ice free conditions over Alaska during the last glaciation (Löfverström and Liakka 2016). In comparison to the model simulations of Löfverström and Liakka (2016) this ridge is weaker in our simulations. Figure 6(a) shows how important the topography is in setting up this feature, and it is absent from the response in the ALB experiment(Figure 3(d)). However, comparing Figure 3(a) and Figure 3(f) shows that the non-linearities introduced by having a dynamic ocean (a feature missing from Löfverström and Liakka 2016) are just as important as topography in causing this feature.

In agreement with previous studies, we find that the summertime response of the stationary wave is predominantly a response to cooling set by the ice sheet's low albedo. There is a small impact of mechanical forcing that acts to amplify the stationary waves as the ice sheet's surface is raised. However, in agreement with Ringler and Cook (1999) the underlying heating field is crucial in setting the response that is then amplified. As was shown by experiment TOP, the effect of topography alone produces the wrong sign of change in the heating field, and consequently the wrong sign in the stationary wave response to the ice sheet.

c. The annual mean

We have discussed the response of the stationary waves in the summer and winter seasons separately. This was motivated by the very different mechanisms known to force the stationary waves in these seasons. To use the evolution of stationary waves as a framework within which to interpret the climate of the past it is often helpful to consider the annual average

response, for this is the timescale upon which some, but by no means all, palaeoclimate proxies record. When looking at the modern climate, Fig. 1 clearly shows that the amplitude of the wintertime stationary waves are significantly larger than those in summertime, thus they dominate the annual mean. In contrast, the anomalies in the stationary waves that we show in response to the ice sheet forcings are equally large in both DJF and JJA (Figs. 2 and 3). Therefore, to understand the *changes* to the annual mean one can not merely consider the changes to the topographically forced winter stationary waves. One must consider the full complexity of the thermally forced summer time circulation as well. Furthermore, upstream of the ice sheet both the winter and summer stationary wave responses are predominantly caused by heating anomalies.

Unavoidably, therefore, when thinking about the annual mean one must take into account the thermally forced behaviour of the stationary waves, not merely the mechanical topographic forcing.

7. The paleoclimate context

In this paper we have emphasised how an ice sheet, which is present all year round, can have a different impact on the atmospheric circulation in the winter and summer seasons. These changes could be reflected at the surface in an altered seasonal cycle. This, in turn could have serious implications for the understanding of paleoclimate proxy records.

On thousand year and longer timescales the seasonal cycle is thought to be affected mostly by changes in the insolation caused by change in the orbital configuration. In particular, the precession of the equinoxes alters the amount of radiation that impinges on the atmosphere in the summer and winter seasons. We have shown that the mechanisms by which the ice sheets affect the climatological stationary waves differ by season. Furthermore, the responses of the circulation to the various mechanisms are also different. This could result in a change to the seasonal cycle of the stationary waves. Since surface climate variables such as temperature,

winds and precipitation are all affected by the stationary waves, palaeoclimate proxies for these variables may also record changes in the seasonal cycle when ice sheets are present. Therefore changes to the seasonal cycle must be interpreted in terms of the ice sheet size as well as the orbital configuration. Similarly, the interpretation of paleoclimate proxies which preferentially record one season must be made with a nod to the influence of ice sheets.

To make this more concrete we present two examples of changes in the surface climate which can only be understood in terms of the season by season changes in the circulation. These are chosen to have general relevance for the understanding of paleoclimate proxies, and are not meant to explain a specific record. We examine the seasonal cycle over Greenland, and changes in the circulation of the North Pacific.

We first consider the temperature over central Greenland. Section 3 shows that in winter, downstream of the White Mountain ice sheet (experiment ALB/TOP) it is the topography that is the most important cause of changes to the stationary waves; Section 4 shows that in summer it is the albedo of the ice sheet that is most important. Figure 2(f) shows that in winter directly over Greenland there is little change in the stationary waves; by contrast, in summer Fig. 3(f) shows that Greenland is affected by a deep anomalous trough. Thus the ice sheet has a different impact on the flow over Greenland in summer and winter. Looking at the summer and winter temperature and wind direction over Greenland will show how these changes in the stationary waves will be felt in surface climate variables. We look first at the surface wind direction, since this variable is the most closely linked to the stationary waves.

Figure 12(a) shows how the wind direction changes over the 21ka to 6ka period as the ice sheet evolves. We see that in winter the wind direction does not appreciably change. In summer, however, there is a 40° shift in the wind direction towards more westerly winds as the upstream ice sheet decays. Such a shift in the winds would have a large impact on the concentration of many of the chemical species, such as the concentration of heavier water isotopes, contained within an ice core. Similarly, Fig. 12(b) shows that as the ice sheet

decays over the deglaciation, the summer temperature over central Greenland increases by up to 3°C. By contrast the winter temperature shows a much smaller change and, indeed, when the 21ka ice sheet is compared to no ice sheet there is no change in the temperature.

This example shows that because the winter and summer stationary wave responses to an ice sheet are different, the seasonal cycle over Greenland is dramatically altered when the LCIS is present. Such a change in the seasonality is important when we consider mass loss from the Greenland ice sheet over the Last Deglaciation. Since mass loss from a retreating ice sheet is driven predominantly by ablation in the summer, the summer warming effect of the retreating LCIS will have a distinct impact on the rate at which mass is lost from the Greenland Ice Sheet (Buizert et al. 2018).

Next we consider the changes to the circulation in the North Pacific and its influence on the tropical Pacific. Jones et al. (2018) showed that there is a significant influence of the LCIS on the climate in Antarctica; this is mediated through the tropics. We show here how this can be understood in terms of the seasonal response of the stationary waves.

Figure 13(b) shows the annual mean response of the near surface winds in the ALB/TOP simulation. This shows that the White Mountain has a strong influence deep into the Tropical Pacific throughout the year. The circulation is typified by a deep cyclone situated in the middle of the North Pacific. We can explain this feature as a summertime response to the albedo of the ice sheet that persists throughout the year due to ocean dynamics, and is further modulated by the the topography of the ice sheet in both winter and summer.

We showed in Section 4, Fig. 3(a), that the presence of the anomalous summer time surface cyclone in the North Pacific is caused by the albedo of the ice sheet. This response occurs in summer without the presence of a dynamic ocean, however, when a dynamic ocean is present, the ocean adjusts to the forcing, allowing the feature to persist throughout year (Fig. 2(d)). The topography of the ice sheet plays a secondary role, altering slightly the circulation forced by the albedo of the ice sheet.

In winter the topography of the ice sheet acts to move the cyclone that formed in the

summer to the south. Figure 2(b) shows that in winter the topography of the ice sheet forces a strong anticyclone that is centred over Alaska. This feature then interacts with the surface cyclone, which results from the SST anomaly caused by the summer circulation, causing it to deepen and move south. Comparing Fig. 2(d) and (f) shows the importance of the ice sheet topography in moving the feature to the south; comparing Fig 2(c) and (f) shows how important the ocean circulation changes, initiated in summer, are. This topographic steering of the cyclone to the south is also apparent in the summer circulation (Fig 3(d) and (f)). We do though emphasise that this purely mechanical topographic effect is an addition to the diabatic heating.

The annual mean response shown in Fig 13(b) is the average of the elements of the responses in winter and summer. As we have described, to understand the impact of the ice sheet on the Pacific circulation we must first understand how the summer circulation is altered by albedo and subsequently how this circulation is altered by the ice sheet's topography. In this way it is possible to understand how the changes in the ice sheet's configuration during the deglaciation can influence the climate of the tropical Pacific as suggested by Russell et al. (2014) and Jones et al. (2018).

These are but two examples of how important it is to understand the seasonal response of the atmospheric circulation to an ice sheet. In attempting to understand paleoclimate proxy records over deglaciations it is necessary to fully appreciate both how the climate responds in different seasons and also how the proxies respond to the seasonal cycle.

a. Other forcing

The experiments that we have described include only changes to the LCIS. During the last glacial period there were other boundary condition changes that we have not analysed. Lowered greenhouse gases could not only have cooled the climate globally, but also altered the meridional temperature gradient (Masson-Delmotte et al. 2006) with a resultant impact on the stationary waves. Previous studies have shown that this is a minor effect (Broccoli

and Manabe 1987), however.

We only consider changes to the topography of the LCIS ignoring the effect of the Eurasian Ice Sheets (EIS). We suggest that the role of the EIS, though locally important, is much smaller than the effect of the LCIS on the global scale. Roe and Lindzen (2001) suggested that the EIS may have an impact on the stationary waves downstream however, this impact would be significantly damped over the Pacific due to the inherent damping in the atmosphere. We have shown that ice sheets can have an upstream impact. However, in the Atlantic, any upstream impact from the EIS will be dwarved by the downstream response of the much larger LCIS: in the Pacific the upstream impacts of the proximal LCIS will also dwarf the downstream effects of the distant EIS. Löfverström et al. (2014) argue that the EIS is located to far north to significantly interact with the westerlies in DJF and also show that the JJA impact is small. Finally, Sherriff-Tadano et al. (2018) explicitly simulate only the impact of the EIS on the climate. They show that although the EIS can have some large local impacts on the climate, on the global scale its impact on the stationary waves is negligible.

We do not consider changes to the orbital configuration. At the LGM this will have a negligible impact since during this period there are minor differences in the orbital parameters compared to today. During the deglacial period, however there are major changes in the orbital configuration. Again we argue that any changes to the climate from the orbital forcing will be much smaller than changes caused by the ice sheets. For example Erb et al. (2015) show that the response of the climate to extremes of ice sheet and orbital forcing differ by almost an order of magnitude.

We thus conclude that because the impact of the LCIS on the atmospheric circulation is so much larger than the impact of other glacial forcings, the results of this study can be applied more generally. Therefore the theoretical framework that we propose is useful for the interpretation of paleoproxy records.

8. Conclusion

In this paper we have described how the atmosphere's stationary waves are affected by the presence of the combined Laurentide Cordilleran Ice Sheet which sat over North America during the last glacial period. We have analysed the mechanisms by which the ice sheet alters the stationary waves elucidating the different summer and winter responses to the albedo and topography of the ice sheet. We use a set of simulations in which we only change the albedo of the surface, a White Plain, in experiment ALB; a set in which we change the topography but leave the surface albedo unchanged, a Green Mountain, in experiment TOP; and a realistic ice sheet in which both the topography and the albedo change, a White Mountain, in experiment ALB/TOP. By analysing the responses to the forcings separately it is possible to understand the combined response to a realistic ice sheet in which both the topography and albedo are different.

In winter the main cause of the changes to the stationary waves from a realistic ice sheet, a White Mountain, is the topography. Downstream of the ice sheet the circulation patterns are very similar for a White Mountain ice sheet and a Green Mountain ice sheet, although the white surface of the White Mountain introduces a diabatic cooling anomaly relative to the Green Mountain which acts to enhance the response. Ocean dynamics also act to enhance the amplitude of the response. Upstream of the ice sheet there are two distinct features. There is an extensive ridge that forms over Alaska which is exclusively a response to topography: its amplitude is unchanged when either the surface albedo is changed or a dynamic ocean is introduced. Farther to the south there are troughs and ridges that form over the Pacific south of 40°N. With the realistic White Mountain ice sheet this is a complex response that involves an interaction between SST anomalies that are established in the North Pacific during the summer, which are a response to the albedo of the ice sheet, and the topographically forced ridge over Alaska. Although complex, this is a robust feature that appears in other climate models (Yanase and Abe-Ouchi 2010). We argue that this pattern is very important for understanding how the LCIS can have a widespread influence on the

climate, even deep into the tropics.

In summer it is the albedo of the surface that has the largest influence on the stationary waves. This implies that the stationary waves are responding to a diabatic heating anomaly. Upstream of the ice sheet the changes to the stationary waves are almost exclusively a response to the albedo over of the ice sheet. There are negligible differences between simulations with either a White Plain or a White Mountain, and those in which we include either a dynamic ocean or those in which we merely specify the SST. This response over the North Pacific is crucial for explaining the wintertime response of the atmosphere in this basin. Over Alaska there is a small topographically forced change in the stationary wave. Downstream of the ice sheet the response of the atmosphere is predominantly caused, again, by the albedo of the ice sheet. However, unlike the upstream response, the topography does play a role. We argue that the impact of the raised topography of a White Mountain compared to a White Plain can be understood as a purely mechanical response to the forcing. However, it must be emphasised that this response is an addition to the diabatic heating changes. For, with a Green Mountain, which causes a diabatic heating anomaly of opposite sign to that caused by the White Mountain, the stationary wave response is also opposite, despite the two ice sheets having the same topography. As in the upstream response we find that ocean dynamics are of negligible importance for understanding the response.

We also showed how the stationary waves respond to a time evolving LCIS over the period of the Last Deglaciation from 6-21 ka. We show that in wintertime it is possible to understand the evolving patterns as a response to the topography. Indeed, we show that the pattern that describes the majority of the variance in the evolution of a White Mountain is the same as that describing the evolution of a Green Mountain. In summertime, by contrast, we find that it is hard to find one single pattern to describe the evolution the White Mountain ice sheet. This fits with our arguments that the response of the summertime stationary waves are a combined response to both albedo and topography.

While our description of the stationary waves responding solely to an ice sheet is inter-

esting from a purely dynamical stand point, it does also have relevance for understanding the climate of the past. We describe two examples where it is possible to extend our understanding of how the atmosphere's stationary waves evolve in summer and winter to problems that may have relevance to paleoclimatologists. These examples are the seasonal cycle over Greenland and the circulation of the North Pacific. These are not meant as the only examples where our results may be of use, rather as examples of how others may apply our results to situations relevant to them.

In understanding changes to the mid-latitude circulation in glacial times the wintertime circulation has received the majority of the attention. In this study we have tried to redress the balance and show that summertime is just as important. For, while the wintertime stationary waves are undoubtedly of larger amplitude than those in summertime, it does not follow that the *changes* in the stationary waves will be larger in winter than in summer. Indeed we show that in some instances the summer season is the most important.

Acknowledgments.

WHGR and PJV were funded by a Leverhulme Trust Research Project Grant. CL was supported by the Research Council of Norway project jetSTREAM (231716)

REFERENCES

Bolin, B., 1950: On the influence of the Earth's orography on the general character of the westerlies. *Tellus*, **2 (3)**, 184–195, doi:10.1111/j.2153-3490.1950.tb00330.x.

Broccoli, A. J. and S. Manabe, 1987: The influence of continental ice, atmospheric CO2, and land albedo on the climate of the last glacial maximum. *Climate Dynamics*, **1 (2)**, 87–99, doi:10.1007/BF01054478.

Buizert, C., B. A. Keisling, J. E. Box, F. He, A. E. Carlson, G. Sinclair, and R. M. DeConto, 2018: Greenland-Wide Seasonal Temperatures During the Last Deglaciation. *Geophysical Research Letters*, **45 (4)**, 1905–1914, doi:10.1002/2017GL075601.

Charney, J. G. and A. Eliassen, 1949: A Numerical Method for Predicting the Perturbations of the Middle Latitude Westerlies. *Tellus*, **1 (2)**, 38–54, doi:10.3402/tellusa.v1i2.8500.

Cook, K. H. and I. M. Held, 1988: Stationary Waves of the Ice Age Climate. *Journal of Climate*, **1 (8)**, 807–819, doi:10.1175/1520-0442(1988)001⟨0807:SWOTIA⟩2.0.CO;2.

Cook, K. H. and I. M. Held, 1992: The Stationary Response to Large-Scale Orography in a General Circulation Model and a Linear Model. *Journal of the Atmospheric Sciences*, **49 (6)**, 525–539, doi:10.1175/1520-0469(1992)049⟨0525:TSRTLS⟩2.0.CO;2.

Donohoe, A., J. Marshall, D. Ferreira, and D. Mcgee, 2013: The Relationship between ITCZ Location and Cross-Equatorial Atmospheric Heat Transport: From the Seasonal Cycle to the Last Glacial Maximum. *Journal of Climate*, **26 (11)**, 3597–3618, doi:10.1175/JCLI-D-12-00467.1.

824 Erb, M. P., C. S. Jackson, and A. J. Broccoli, 2015: Using single-forcing GCM sim-
825 ulations to reconstruct and interpret Quaternary climate change. *Journal of Climate*,
826 151001105425005, doi:10.1175/JCLI-D-15-0329.1.

827 European Centre for Medium-Range Weather Forecasts, 2012: {ERA-I}nterim Project,
828 Monthly Means. Research Data Archive at the National Center for Atmospheric Research,
829 Computational and Information Systems Laboratory, doi:10.5065/D68050NT.

830 Gordon, C., C. Cooper, C. A. Senior, H. Banks, J. M. Gregory, T. C. Johns, J. F. B.
831 Mitchell, and R. A. Wood, 2000: The simulation of SST, sea ice extents and ocean heat
832 transports in a version of the Hadley Centre coupled model without flux adjustments.
833 *Climate Dynamics*, **16 (2-3)**, 147–168, doi:10.1007/s003820050010.

834 Hartmann, D. L., 1994: *Global Physical Climatology*. International Geophysics, Elsevier
835 Science.

836 Held, I. M., 1983: Stationary and quasi-stationary eddies in the extratropical troposphere:
837 theory. *Large-scale Dynamical Processes in the Atmosphere*, Academic Press, London,
838 1949, 127–168.

839 Held, I. M., M. Ting, and H. Wang, 2002: Northern winter stationary waves: Theory and
840 modeling. *Journal of Climate*, **15 (16)**, 2125–2144, doi:10.1175/1520-0442(2002)015⟨2125:
841 NWSWTA⟩2.0.CO;2.

842 Hofer, D., C. C. Raible, a. Dehnert, and J. Kuhlemann, 2012: The impact of different glacial
843 boundary conditions on atmospheric dynamics and precipitation in the North Atlantic
844 region. *Climate of the Past*, **8 (3)**, 935–949, doi:10.5194/cp-8-935-2012.

845 Hoskins, B. J. and T. Ambrizzi, 1993: Rossby Wave Propagation on a Realistic Longi-
846 tudinally Varying Flow. *Journal of the Atmospheric Sciences*, **50 (12)**, 1661–1671, doi:
847 10.1175/1520-0469(1993)050⟨1661:RWPOAR⟩2.0.CO;2.

Hoskins, B. J. and D. J. Karoly, 1981: The Steady Linear Response of a Spherical Atmosphere to Thermal and Orographic Forcing. *Journal of the Atmospheric Sciences*, **38 (6)**, 1179–1196, doi:10.1175/1520-0469(1981)038⟨1179:TSLROA⟩2.0.CO;2.

Hoskins, B. J. and M. J. Rodwell, 1995: A Model of the Asian Summer Monsoon. Part I: The Global Scale. *Journal of the Atmospheric Sciences*, **52 (9)**, 1329–1340, doi:10.1175/1520-0469(1995)052⟨1329:AMOTAS⟩2.0.CO;2.

Jackson, C., 2000: Sensitivity of stationary wave amplitude to regional changes in Laurentide ice sheet topography in single-layer models of the atmosphere. *Journal of Geophysical Research*, **105 (D19)**, 24 443, doi:10.1029/2000JD900377.

Jones, T. R., W. H. G. Roberts, E. J. Steig, K. M. Cuffey, B. R. Markle, and J. W. C. White, 2018: Southern Hemisphere climate variability forced by Northern Hemisphere ice-sheet topography. *Nature*, **554**, 351–355, doi:10.1038/nature24669.

Kageyama, M. and P. J. Valdes, 2000: Impact of the North American ice-sheet orography on the Last Glacial Maximum eddies and snowfall. *Geophysical Research Letters*, **27 (10)**, 1515–1518, doi:10.1029/1999GL011274.

Kageyama, M., et al., 2017: The PMIP4 contribution to CMIP6 Part 4: Scientific objectives and experimental design of the PMIP4-CMIP6 Last Glacial Maximum experiments and PMIP4 sensitivity experiments. *Geoscientific Model Development*, **10**, 4035–4055, doi:10.5194/gmd-10-4035-2017.

Löfverström, M., R. Caballero, J. Nilsson, and J. Kleman, 2014: Evolution of the large-scale atmospheric circulation in response to changing ice sheets over the last glacial cycle. *Climate of the Past*, **10 (4)**, 1453–1471, doi:10.5194/cp-10-1453-2014.

Löfverström, M., R. Caballero, J. Nilsson, and G. Messori, 2016: Stationary Wave Reflection as a Mechanism for Zonalizing the Atlantic Winter Jet at the LGM. *Journal of the Atmospheric Sciences*, **73 (8)**, 3329–3342, doi:10.1175/JAS-D-15-0295.1.

Löfverström, M. and J. Liakka, 2016: On the limited ice intrusion in Alaska at the LGM. *Geophysical Research Letters*, **43 (20)**, 11,030–11,038, doi:10.1002/2016GL071012.

Manabe, S. and a. J. Broccoli, 1985: The influence of continental ice sheets on the climate of an ice age. *Journal of Geophysical Research*, **90 (D1)**, 2167, doi:10.1029/JD090iD01p02167.

Masson-Delmotte, V., et al., 2006: Past and future polar amplification of climate change: Climate model intercomparisons and ice-core constraints. *Climate Dynamics*, **26 (5)**, 513–529, doi:10.1007/s00382-005-0081-9.

Merz, N., C. C. Raible, and T. Woollings, 2015: North Atlantic eddy-driven jet in interglacial and glacial winter climates. *Journal of Climate*, **28 (10)**, 3977–3997, doi:10.1175/JCLI-D-14-00525.1.

Nigam, S., I. M. Held, and S. W. Lyons, 1986: Linear Simulation of the Stationary Eddies in a General Circulation Model. Part I: The No-Mountain Model. *Journal of the Atmospheric Sciences*, **43 (23)**, 2944–2961, doi:10.1175/1520-0469(1986)043⟨2944:LSOTSE⟩2.0.CO;2.

Nigam, S., I. M. Held, and S. W. Lyons, 1988: Linear Simulation of the Stationary Eddies in a GCM. Part II: The Mountain Model. *Journal of the Atmospheric Sciences*, **45 (9)**, 1433–1452, doi:10.1175/1520-0469(1988)045⟨1433:LSOTSE⟩2.0.CO;2.

Otto-Bliesner, B. L., E. C. Brady, G. Clauzet, R. Tomas, S. Levis, and Z. Kothavala, 2006: Last glacial maximum and holocene climate in CCSM 3. *Journal of Climate*, **19 (11)**, 2526–2544, doi:10.1175/JCLI3748.1.

Pausata, F. S. R., C. Li, J. J. Wettstein, M. Kageyama, and K. H. Nisancioglu, 2011: The key role of topography in altering North Atlantic atmospheric circulation during the last glacial period. *Climate of the Past*, **7 (4)**, 1089–1101, doi:10.5194/cp-7-1089-2011.

Peixoto, J. P., A. H. Oort, E. N. Lorenz, and A. I. of Physics, 1992: *Physics of Climate*. American Inst. of Physics.

Peltier, W. R., 2004: Global Glacial Isostasy and the Surface of the Ice-age Earth: The ICE-5G (VM2) Model and GRACE. *Annual Review of Earth and Planetary Sciences*, **32 (1)**, 111–149, doi:10.1146/annurev.earth.32.082503.144359.

Pope, V. D., M. L. Gallani, P. R. Rowntree, and R. a. Stratton, 2000: The impact of new physical parametrizations in the Hadley Centre climate model: HadAM3. *Climate Dynamics*, **16 (2-3)**, 123–146, doi:10.1007/s003820050009.

Ringler, T. D. and K. H. Cook, 1999: Understanding the Seasonality of Orographically Forced Stationary Waves: Interaction between Mechanical and Thermal Forcing. *Journal of the Atmospheric Sciences*, **56 (9)**, 1154–1174, doi:10.1175/1520-0469(1999)056⟨1154:UTSOOF⟩2.0.CO;2.

Roberts, W. H. G. and P. J. Valdes, 2017: Green mountains and white plains: The effect of northern hemisphere ice sheets on the global energy budget. *Journal of Climate*, **30 (10)**, 3907–3925, doi:10.1175/JCLI-D-15-0789.1.

Rodwell, M. J. and B. J. Hoskins, 2001: Subtropical anticyclones and summer monsoons. *Journal of Climate*, **14 (15)**, 3192–3211, doi:10.1175/1520-0442(2001)014⟨3192:SAASM⟩2.0.CO;2.

Roe, G. H. and R. S. Lindzen, 2001: The Mutual Interaction between Continental-Scale Ice Sheets and Atmospheric Stationary Waves. *Journal of Climate*, **14 (7)**, 1450–1465, doi:10.1175/1520-0442(2001)014⟨1450:TMIBCS⟩2.0.CO;2.

Russell, J. M., et al., 2014: Glacial forcing of central Indonesian hydroclimate since 60,000 y B.P. *Proceedings of the National Academy of Sciences of the United States of America*, **111 (14)**, 5100–5, doi:10.1073/pnas.1402373111.

Sherriff-Tadano, S., A. Abe-Ouchi, M. Yoshimori, A. Oka, and W.-L. Chan, 2018: Influence of glacial ice sheets on the Atlantic meridional overturning circulation through surface wind change. *Climate Dynamics*, **50 (7-8)**, 2881–2903, doi:10.1007/s00382-017-3780-0.

Smagorinsky, J., 1953: The dynamical influence of large-scale heat sources and sinks on the quasi-stationary mean motions of the atmosphere. *Quarterly Journal of the Royal Meteorological Society*, **79 (341)**, 342–366, doi:10.1002/qj.49707934103.

Ting, M. F., 1994: Maintenance of Northern Summer Stationary Waves in a Gcm. *Journal of the Atmospheric Sciences*, **51 (22)**, 3286–3308, doi:Doi10.1175/1520-0469(1994)051⟨3286:Monssw⟩2.0.Co;2.

Ullman, D. J., A. N. Legrande, A. E. Carlson, F. S. Anslow, and J. M. Licciardi, 2014: Assessing the impact of laurentide ice sheet topography on glacial climate. *Climate of the Past*, **10 (2)**, 487–507, doi:10.5194/cp-10-487-2014.

Valdes, P. J. and B. J. Hoskins, 1989: Linear Stationary Wave Simulations of the Time-Mean Climatological Flow. *Journal of the Atmospheric Sciences*, **46 (16)**, 2509–2527, doi:10.1175/1520-0469(1989)046⟨2509:LSWSOT⟩2.0.CO;2.

Valdes, P. J., et al., 2017: The BRIDGE HadCM3 family of climate models: HadCM3@Bristol v1.0. *Geoscientific Model Development*, **10 (10)**, 3715–3743, doi:10.5194/gmd-10-3715-2017.

Yanase, W. and A. Abe-Ouchi, 2010: A numerical study on the atmospheric circulation over the midlatitude North Pacific during the last glacial maximum. *Journal of Climate*, **23 (1)**, 135–151, doi:10.1175/2009JCLI3148.1.

List of Tables

	DJF		JJA	
	upstream	downstream	upstream	downstream
ALB	66 (0.80)	53 (0.92)	92 (0.99)	89 (0.99)
TOP	91 (0.99)	92 (0.99)	89 (0.99)	94 (0.99)
ALB/TOP	95 (0.99)	93 (0.99)	84 (0.99)	86 (0.98)

TABLE 1. Percentage of variance captured by the first EOF of 200 hPa height, and, in brackets, pattern correlation with the 21ka stationary waves for 21-6ka suite of simulations

List of Figures

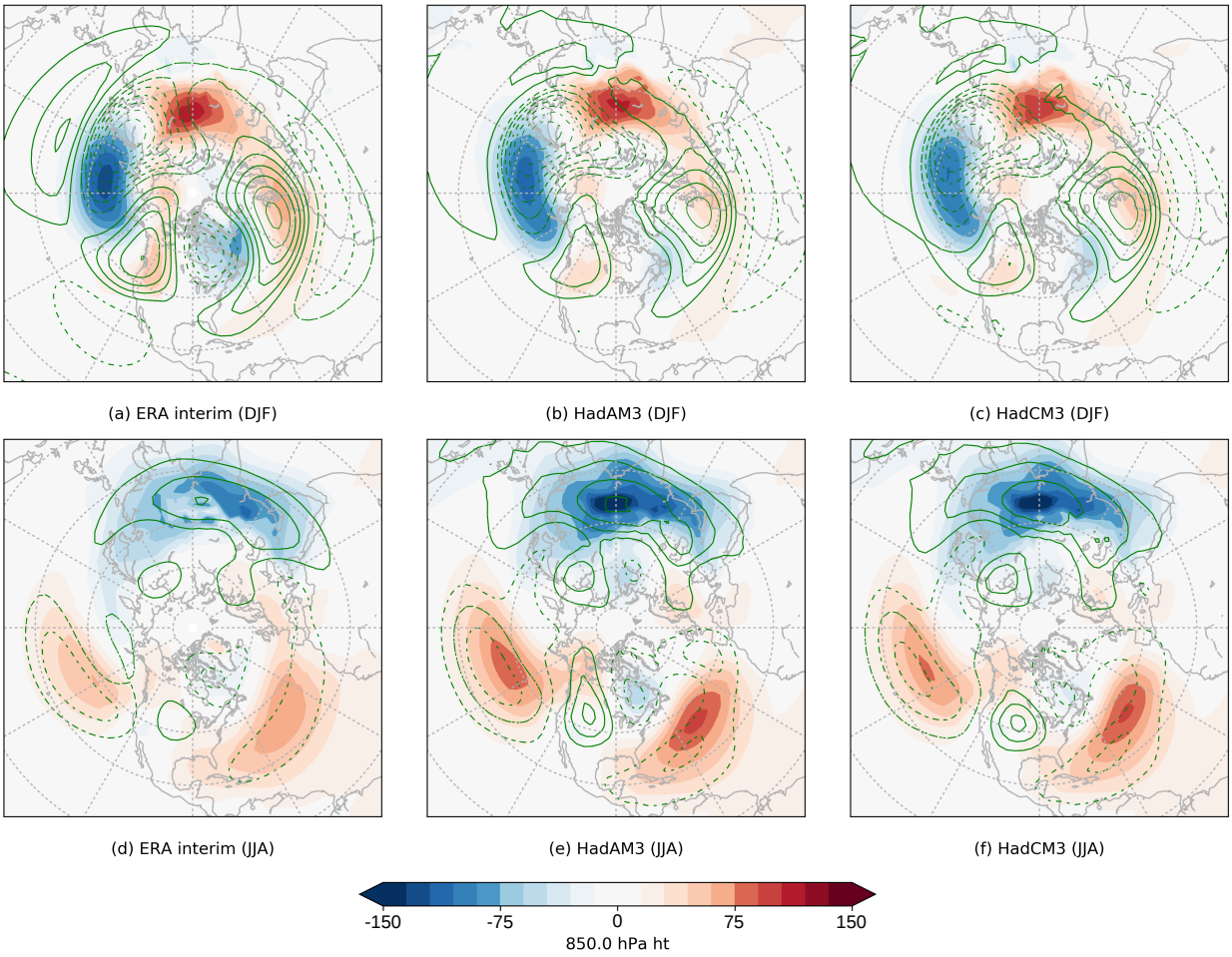

FIG. 1. Geopotential height at surface and upper levels for control simulations. Eddy z200 (contours) and z850 (colours) for ERA-interim (observations, a,d), HadAM3 (atmosphere-only, b,e), HadCM3 (coupled, d,f) in the DJF (a,b,c) and JJA (d,e,f) seasons. Contours change every 40m, dashed contours indicate negative values. Colours change every 15m.

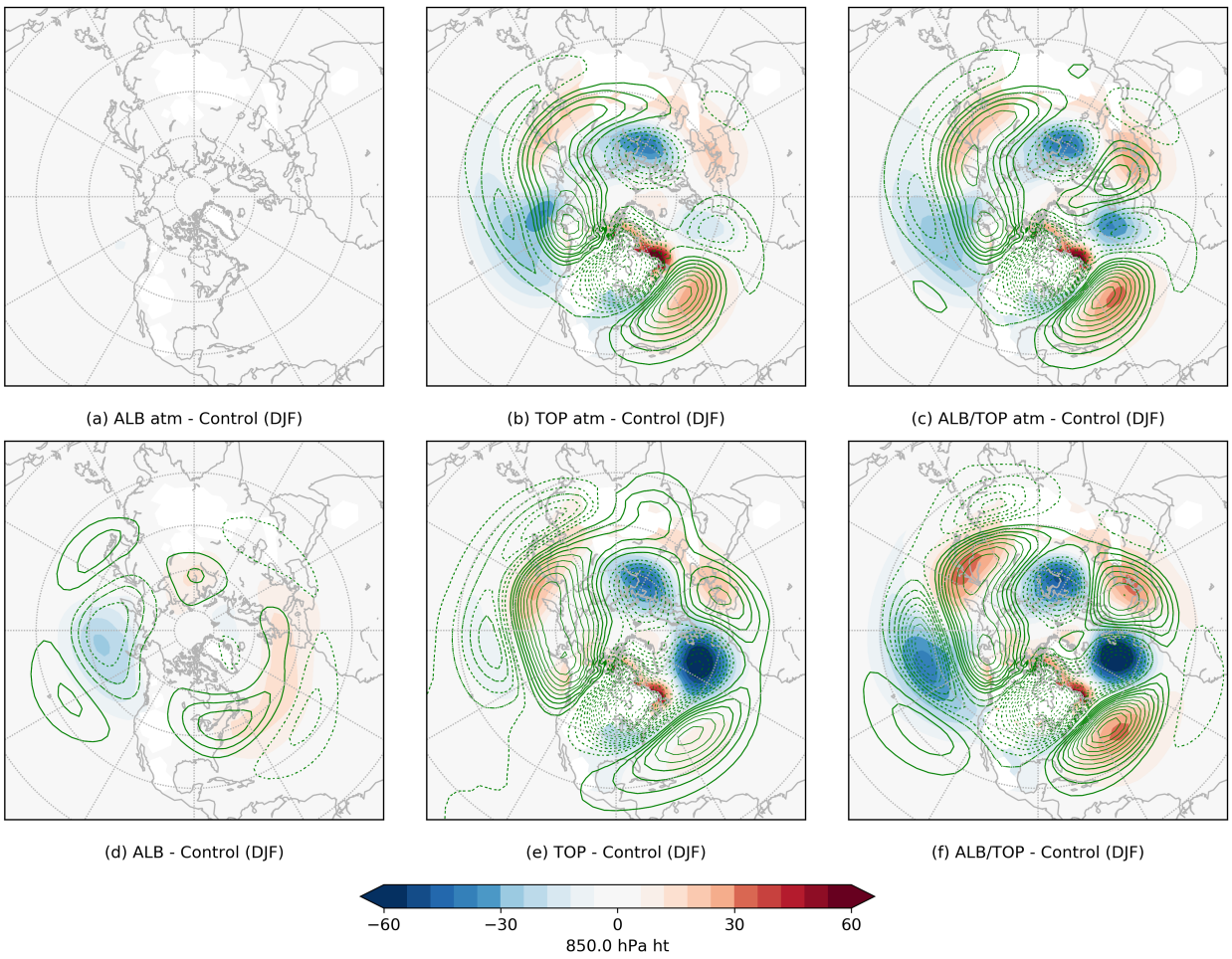

FIG. 2. Difference between the ice sheet and control simulation eddy z200 (contours), and z850 (colours) during DJF. Top row atmosphere-only simulations, bottom row coupled simulations. Panels (a,d) show experiment ALB, (b,e) experiment TOP, (c,f) experiment ALB/TOP. Contours change every 10m, dashed contours indicate negative values. Colours change every 6m.

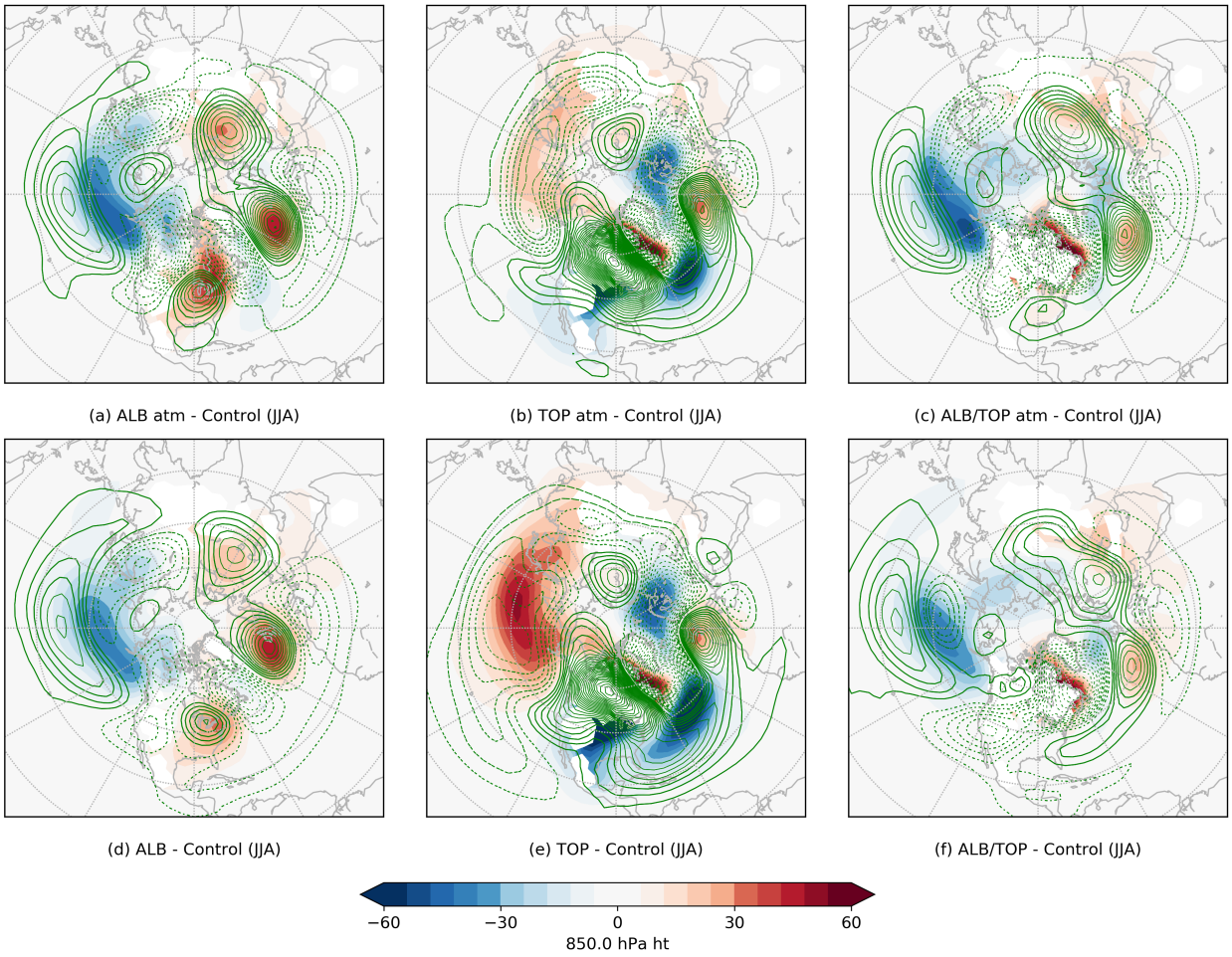

FIG. 3. Difference between the ice and control simulation eddy z200 (contours), and z850 (colours) during JJA. Plotting as in Fig. 2.

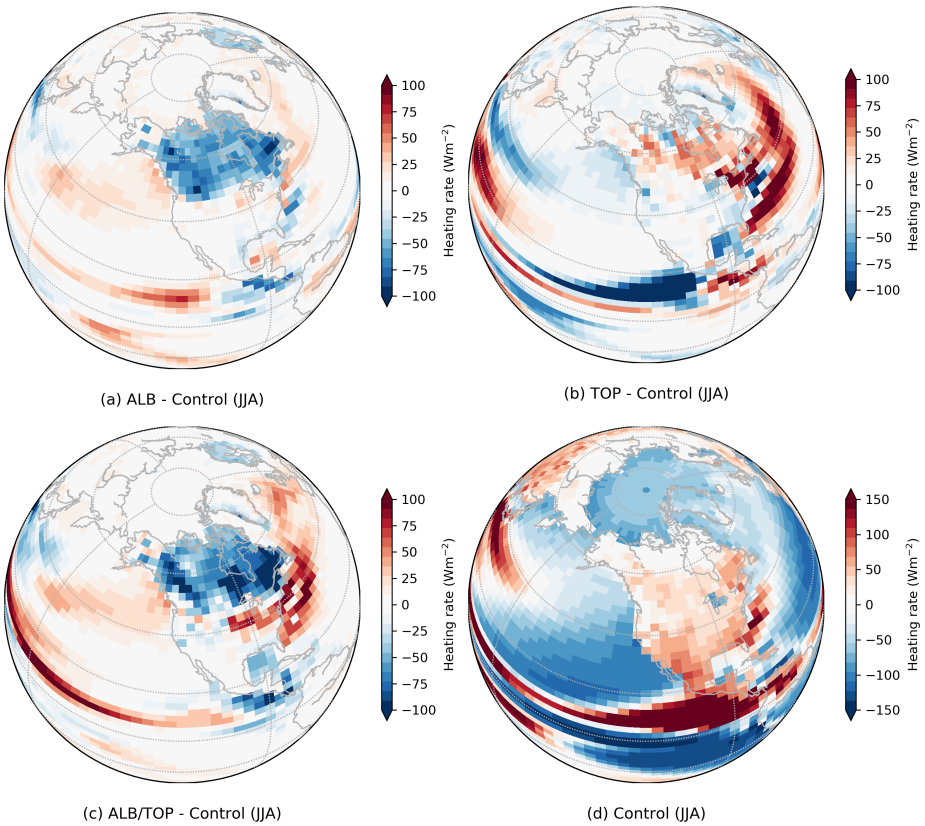

FIG. 4. Difference between the JJA diabatic heating field for the ice sheet and the control simulation (a, b, c). (d) shows the control simulation diabatic heating. Colours change every 10 W m^{-2}.

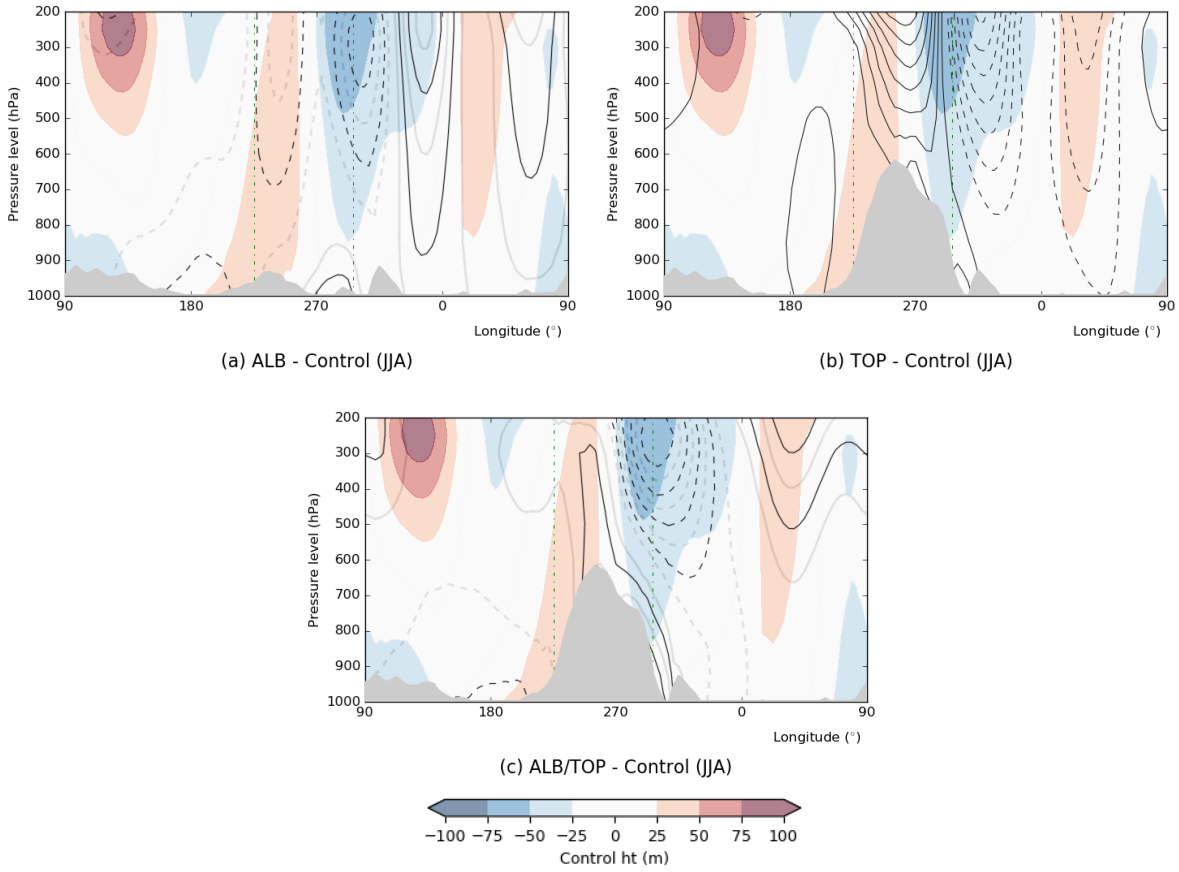

FIG. 5. Vertical section of the change in the JJA eddy geopotential height averaged between 50°-70°N. (a) shows experiment ALB, (b) TOP, (c) ALB/TOP. Colours show the control eddy height field, contours show the anomalies for each experiment relative to the control. The contour interval is 25(m) for both colours and contours, negative contours are shown by the dashed lines (faint grey contours show intermediate, 12.5m contours in panels (a) and (c)). The green vertical dash-dotted lines indicate the western and eastern edges of the ice sheet, the greyed out regions show the surface topography.

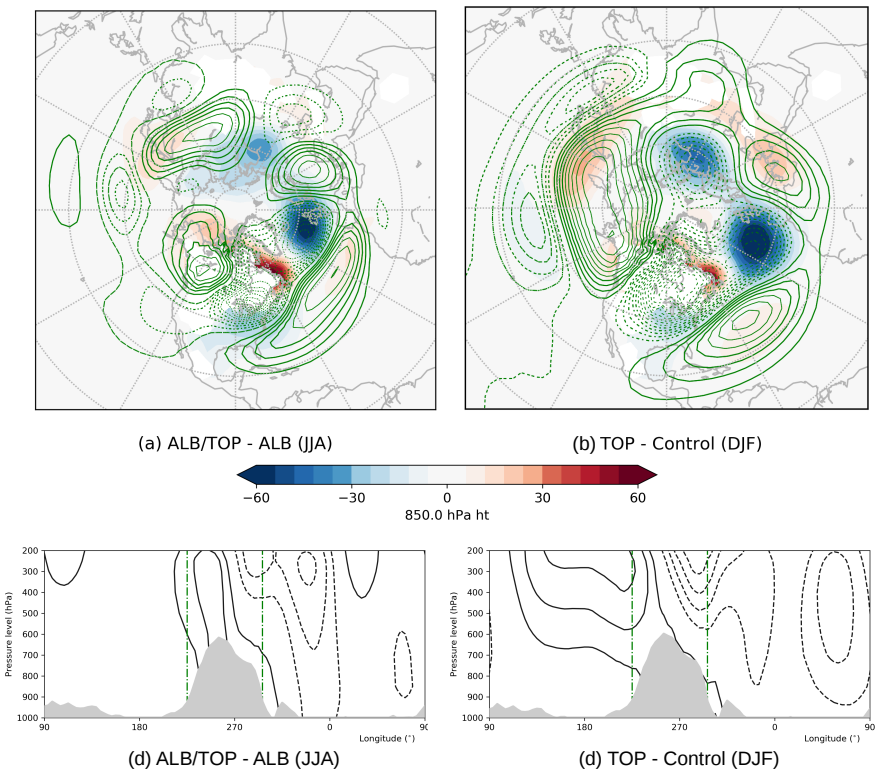

FIG. 6. Effect of an elevated white surface in JJA. Top panels show maps of the change in the eddy z200 (contours) and z850 (colours) height fields. Bottom to panels show vertical sections of the eddy height field averaged between 50-70°N. Left column shows the difference between ALB/TOP and ALB in JJA, right column shows difference between TOP and Control in DJF. In the upper panels (a) and (b) the contours change every 40m, dashed contours indicate negative values, colours change every 15m. In the lower panels (c) and (d) the contour interval is 25(m) for both colours and contours, negative contours are shown by the dashed lines. The green vertical dash-dotted lines indicate the western and eastern edges of the ice sheet, the greyed out regions show the surface topography.

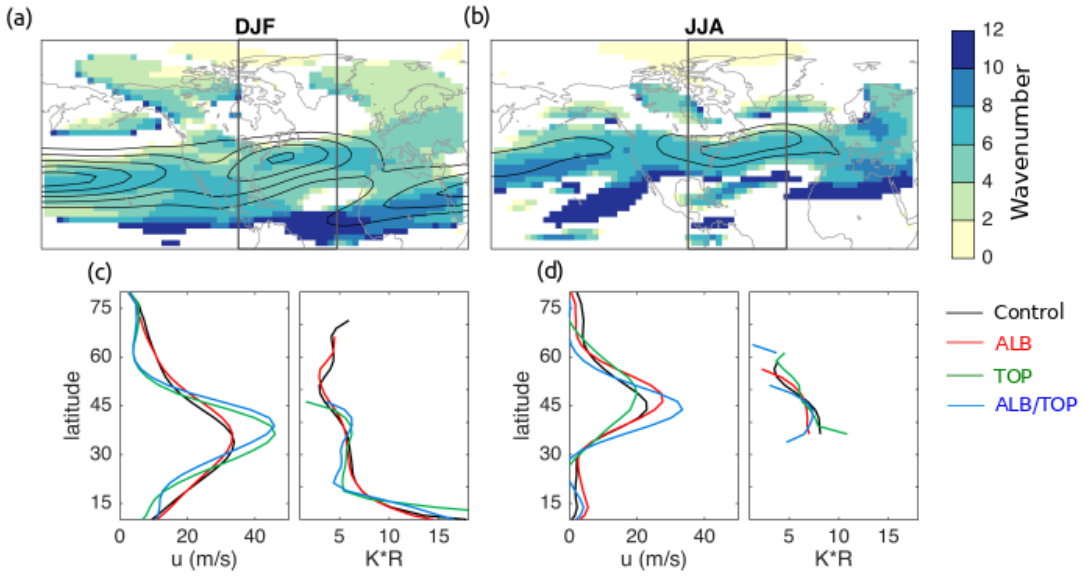

FIG. 7. Planetary wavenumbers for various simulations. Panels (a,b) show maps of the stationary wavenumber for the simulations ALB/TOP in DJF (a) and JJA (b), contours show the zonal wind speed. Panels (c,d) show on the right sections of the stationary wavenumber against latitude in the Atlantic basin (the region marked by the box in the upper panels); on the left the average zonal wind. In all panels, the stationary wave numbers are calculated as an average for phase speeds between 3-7 ms^{-1}.

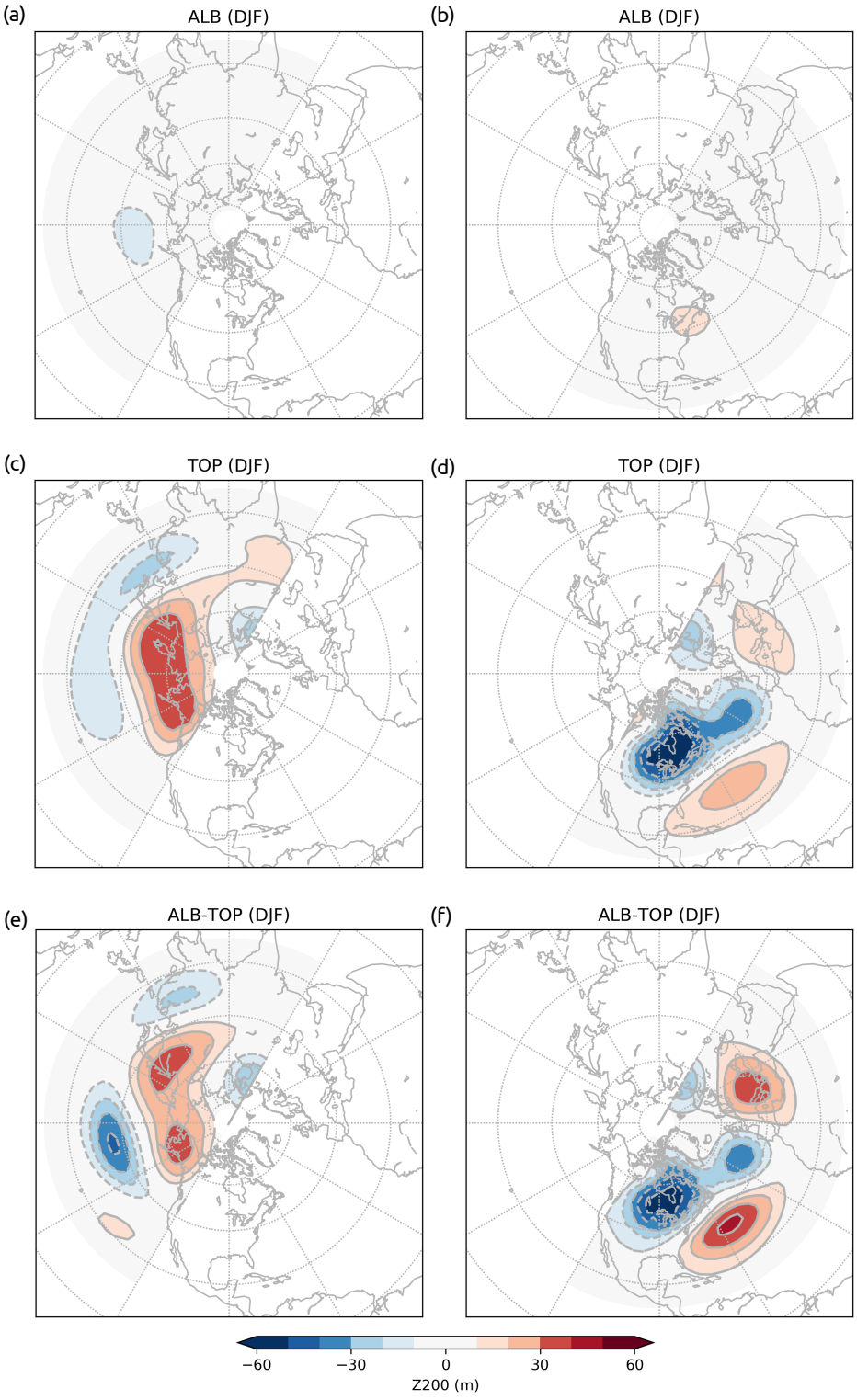

FIG. 8. EOFs of 200 hPa height for DJF computed over the period 21ka-6ka. Left hand set of panels show EOFs computed from 120°W to 60°E, right hand set of panels for 60°E to 240°E. Units are meters

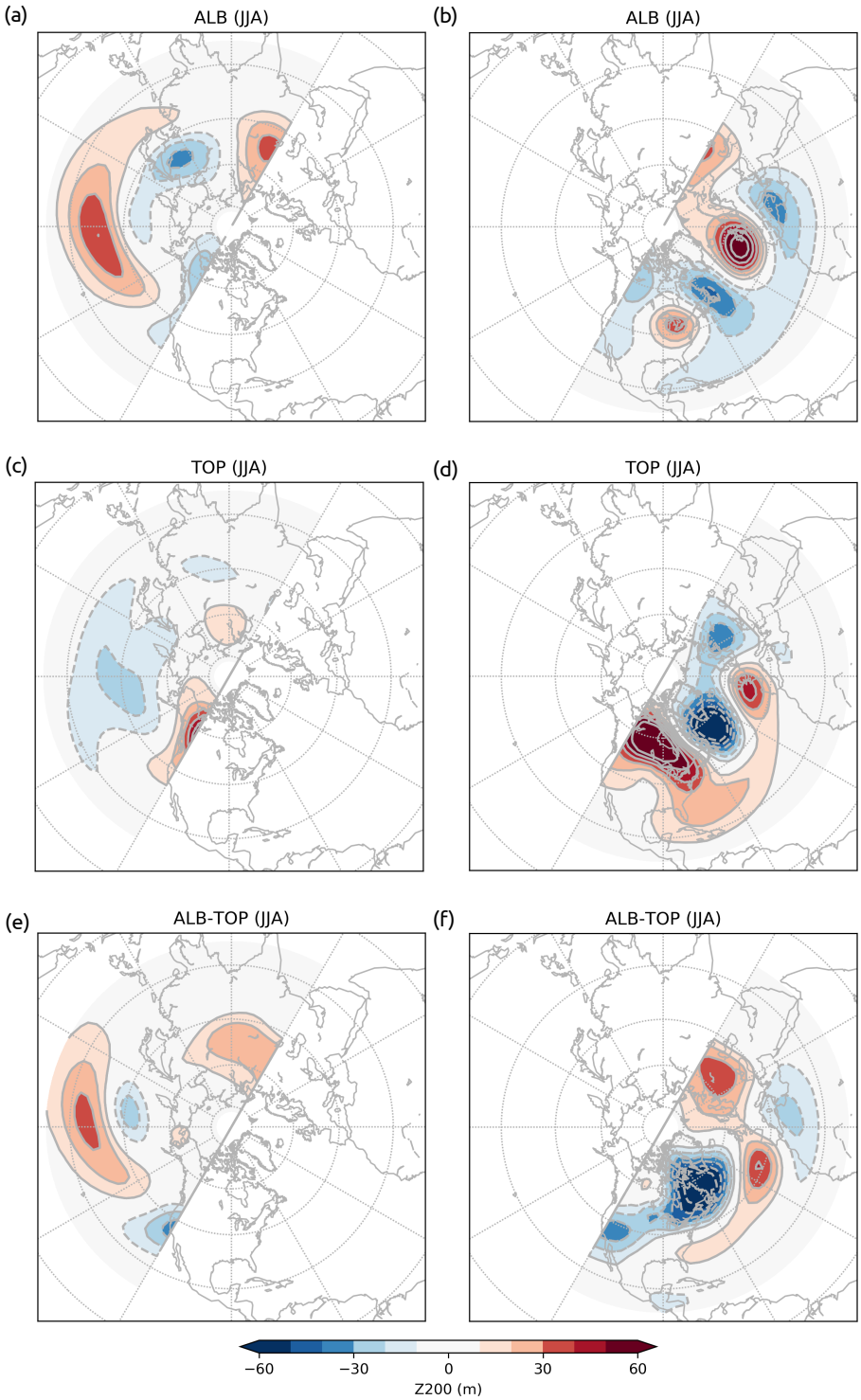

FIG. 9. EOFs of 200 hPa height for JJA computed over the period 21ka-6ka. Plotting as for Fig. 8

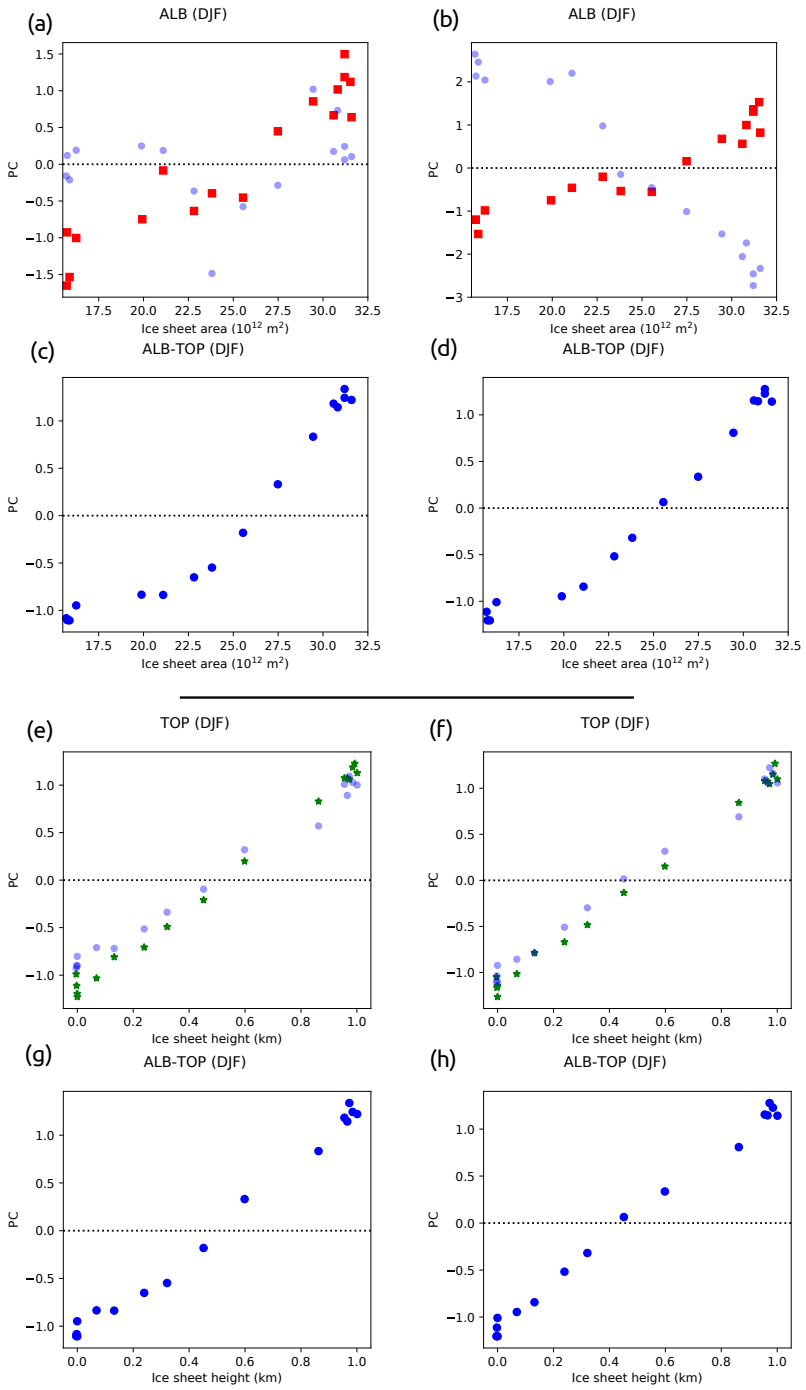

FIG. 10. Principal components of 200 hPa height for DJF computed over the period 21ka-6ka plotted against the area and height of the ice sheet. The left hand column shows the PC for the upstream EOF (120°W to 60°E) the right hand column for the downstream PCs (60°E to 240°E). The top four panels plot PCs of ALB (a,b) and ALB/TOP (c,d) against the area of the ice sheet, the lower four panels plot the PCs of TOP (e,f) and ALB/TOP (g,h) against the mean height of the ice sheet. The light blue circles shown for experiments ALB and TOP are computed by projecting the EOFs from each experiment onto the 200hPa height field from experiment ALB-TOP. Thus the light circles in (a,b) are those computed in exactly as in Equation 2, in (e,f) they are computed for experiment TOP.

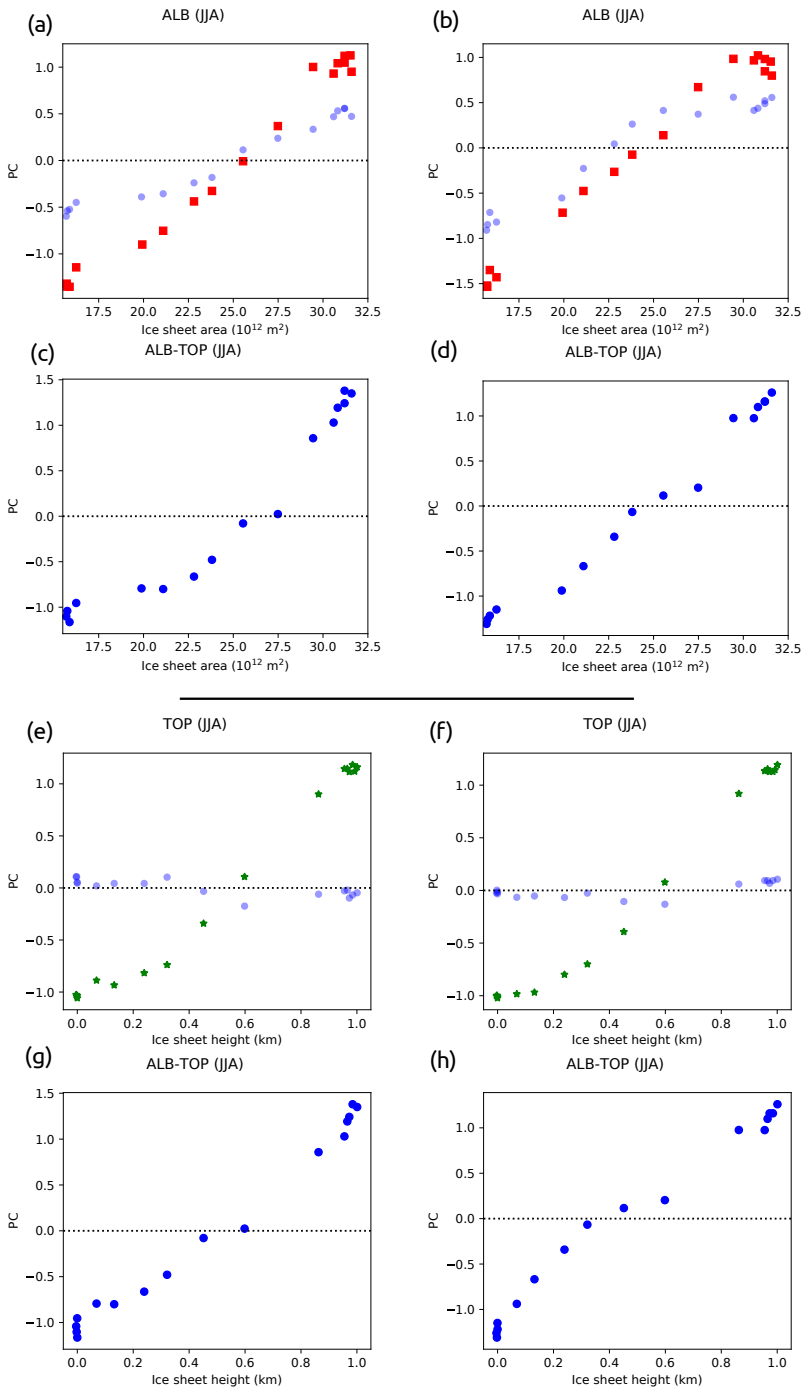

FIG. 11. Principal components of 200 hPa height for JJA computed over the period 21ka-6ka plotted against the area and height of the ice sheet. Plotting as for Fig. 10

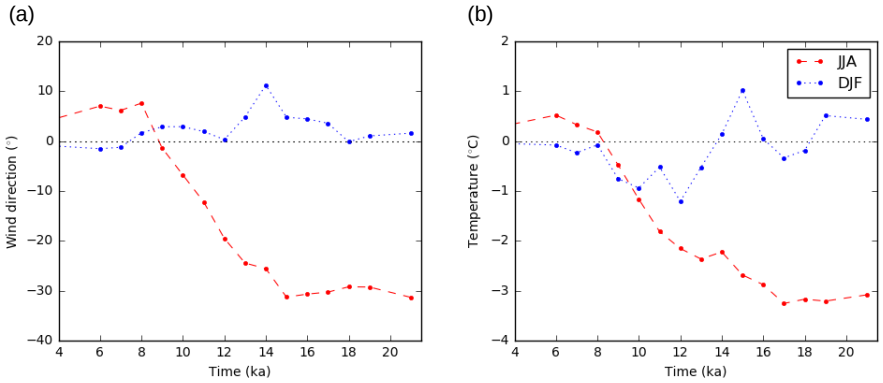

FIG. 12. Change in the wind direction (a) and temperature (b) over central Greenland for the ALB/TOP suite of simulations relative to the control pre-industrial simulation. Blue dashed line shows the JJA average, orange dotted line shows the DJF average. The time is the time for which the ice sheet reconstruction is made.

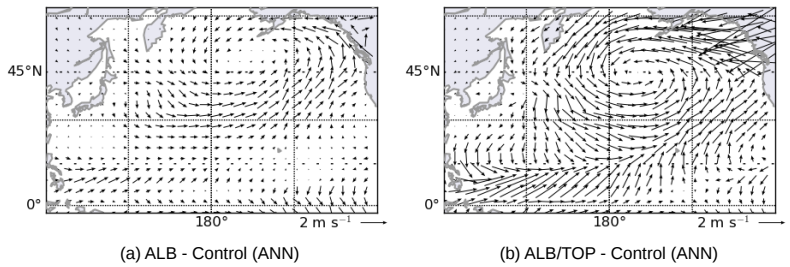

(a) ALB - Control (ANN) (b) ALB/TOP - Control (ANN)

FIG. 13. Change in the annual mean 10m wind in the North Pacific for experiment ALB (a) and ALB/TOP (b).